Republic of Iraq
Ministry of Higher Education
& Scientific Research
University of Babylon
College of Education for Pure Sciences
Department of Physics

Preparation and Characterization of ($PVA-Y_2O_3$) nanocomposites

A Thesis
Submitted to the Council of the College of Education for Pure Sciences of University of Babylon in Partial Fulfillment of the Requirements for the Degree of Master in Education / Physics

By

Ali Jabbar Louis Abdullah
B.Sc. In Physics, University of Babylon (2017)

Supervised by

Prof. Dr. Ali Razzaq Abdulridha
College of Education for Pure Sciences
Department of Physics

2023 A.D. **1445 A.H.**

بسم الله الرحمن الرحيم

وَيَسْأَلُونَكَ عَنِ الرُّوحِ قُلِ الرُّوحُ مِنْ أَمْرِ رَبِّي وَمَا
أُوتِيتُمْ مِنَ الْعِلْمِ إِلَّا قَلِيلًا

صدق الله العلي العظيم

(سورة الإسراء/ آية ٨٥)

To my family

Acknowledgementi

Praise be to ALLAH , Lord of the whole creation and peace be upon his messenger Mohammad and his family .

My especial appreciation to my supervisor Prof. Dr. Ali Razzaq Abdulridha, for suggesting this project, help, guidance and advice, throughout the work and for many helpful discussions and suggestions. His understanding and expertise in my area of research greatly improved the contents of this thesis .

I am grateful to the Dean of the College of Education for Pure Sciences and the staff members of the Physics department for their help and kind assistance.

Last but not least, I extend my thanks and appreciation to my family for their support to me for the duration of the study.

Ali

Summary

In this study, the un-doped and PVA doped Y_2O_3 nanoparticles nanocomposite films were prepared using solution casting method with variant content of (Y_2O_3)nanoparticles (0, 1.5, 3, 4.5 and 6) wt.%. The structural, morphological and structure, optical and AC electrical properties of PVA and (PVA/Y_2O_3) nanocomposites have been investigated. The Morphology properties include optical microscope (OM), Fourier transformation infrared ray (FTIR). The optical microscope images show that Y_2O_3 nanoparticles form a continuous network inside the polymers when the ratio of (6) wt.%. FTIR spectra show a shift in some bands and change in the intensities of others band comparing with pure (PVA) polymer, this indicates there is physical interaction between the polymers and the added nanoparticle. The optical properties exhibited that the absorbance, absorption coefficient, refractive index, extinction coefficient, dielectric constant (real and imaginary) and optical conductivity of (PVA/Y_2O_3) nanocomposites increased with the increasing of the concentrations of the (Y_2O_3) nanoparticles. The transmittance and the energy gap for indirect transition (allowed and forbidden) decreased with the increasing of the concentrations of (Y_2O_3) nanoparticles.The AC electrical properties exhibited that the dielectric constant and dielectric loss for (PVA/Y_2O_3) nanocomposites were increased with the increasing of (Y_2O_3) nanoparticles concentration and decreasing with the increase of frequency of the applied electric field. The A.C electrical conductivity increased with the increasing of (Y_2O_3) nanoparticles concentration and frequency of the applied electric field frequency.

Contents

List of Symbols

Symbol	Physical meaning
σ_{op}	Optical conductivity
σ_{AC}	Alternative current electric conductivity
E_{ele}	Electronic energy
E_{vib}	Vibration energy
E_{rot}	Rotation energy
E_{tran}	Transitional energy
ϑ	Wavenumber
λ	Wavelength
A	Absorbance
T	Transmittance
R	Reflectance
I_A	Absorbed light intensity
I_o	Incident light intensity
Eg^{opt}	Optical energy gap
E_{ph}	Energy of photon
t	Thickness of the matter
α	Absorption coefficient
f	Frequency
V	Voltage
V_m	Maximum voltage
ω	angular frequency
n	Refractive Index
N	Complex Refractive Index
C	Capacitance of a capcitor
C_p	Capacitor containing an insulator material

$\mathcal{E}_1$	Real part of Dielectric constant
$\mathcal{E}_2$	Imaginary part of Dielectric constant
h	Plank constant
$tan\delta$	Loss Factor
ε'	Dielectric constant
ε''	Dielectric loss
E_g	Energy gap
v	Light speed in matter
c	Light speed in vacuum
k	Extinction coefficient
I	Current
I_p	Conduction Current
I_q	Capacitates current
d	thickness
A_r	Area
R_p	Resistance at low frequencies

List of Figures

List of Tables

List of Abbreviations

Symbol	Physical MEANING
PVA	Polyvinyl Alcohol
NPs	Nanocomposites
Y_2O_3	Yttrium Oxide

Chapter One

Introduction and Literature Review

1.1 Introduction

In limited to recent years, the use of most polymers was recent years the manufacture of cheap products which were used for simple purposes. However, the speedy technical development has required the replacement of some materials being used in industry with others having better specifications. The polymers have replaced iron and aluminum for some purposes that require high temperature and stress [1].

Polymer composites have unrivaled properties like light weight, high flexibility, and possibility to be produced at low temperature and low cost [2]. The polymers can be divided into there: industrial and natural. The natural polymers include proteins, cellulose, starches and rubber, either the industrial polymers include polyvinyl chloride, polypropylene, nylons polyethylene, Polyvinyl Alcohol, Polyacrylamide and polyesters polycarbonate, etc.[3]. Over the past few years, a little word with big potential has been rapidly insinuating itself into the world's consciousness, that word is "Nano". Nanotechnology is one of the leading scientific fields today since it combines knowledge from the fields of physics, chemistry, biology, medicine, informatics, and engineering. It is an emerging technological field with great potential to lead in great breakthroughs that can be applied in real life. Nanotechnology tools and techniques enable the fabrication and control of new nano and biomaterials, as well as nanodevices [4].

Nanotechnology, often known as nanoscale science, is the study of matter at the nanoscale, which is defined as the range of (1 to 100) nm. A breakthrough in academic and industrial interest in these nanomaterials over the past 10 years has been of interest due to the remarkable differences in solid-state properties. In Greek, "Nano" means little man, while the SI unit "Nano" corresponds to (10^{-9} m) magnitudes, such as nanometers, nanoliters, nanograms [5].

The nanosciences have attracted a lot of interest for a number of reasons. Among them, the very large surface to volume ratio showed by many nanoscaled materials opened novel possibilities in surface-based science, such as heterogeneous catalysis [6].

Moreover, it has been discovered that the properties of materials change as their size approaches the nanoscale, or when a portion of certain atoms on the material's surface becomes significant. For example, inert metals such as platinum can act as catalysts, semiconductors such as silicon can act as conductors that become conductive, etc., the applications of nanotechnology have only increased in recent years, and the highest potential application is in the field of materials, followed by electronics and medicine [7].

1.2 Polymer Structure

Polymers are large organic molecules (macromolecules) composed of small structural components (monomers) linked together in a polymerization process [8]. Polymers with low temperatures have limited crystal connections because polymers are made up of big, linked molecules that are difficult to handle. A linear chain of molecules can only arrange itself in an orderly fashion in a few locations. In the solid state, polymers have crystalline and non-crystalline regions [9].

1.3 Classification of Polymers

1.3.1 Chemical classification of polymers

There are different kinds of polymers categorized according to their structure and as follows [9] [10]:

1.3.1.1 Linear polymers

Single molecular is the basic structural unit for polymers in a series of certain lengths that are connected in a linear form. Linear polymers may include

totals twisted that are a part of monomer but without any branch, as revealed in figure (1.1a).

1.3.1.2 Branched polymers

This type of polymers consists of several branches that could be a Ladder and Crusader or Comb, which is usually present with various lengths, as illustrated in Figure (1.1 b).

1.3.1.3 Cross linked polymers

This kind of polymers consists of chains from three dimensional linked together in more than one site and monomers bonding in effective totals that are chemical bonds, as displayed in Figure (1.1 c).

1.3.1.4 Network polymers

Three-dimensional (3D) networks are made of trifunctional. Examples: phenol-formaldehyde and epoxies, such as in the Figure (1.1d).

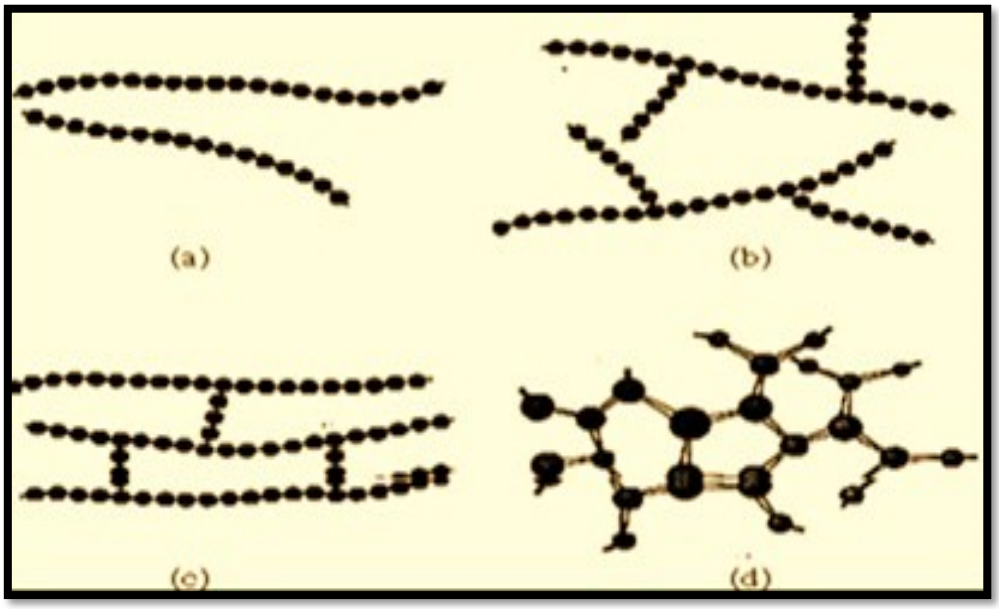

Figure (1.1): Polymeric chains types (A) linear, (B) branched, (C) cross-linked and (D) network polymers [11].

1.3.2 Thermal classification of polymers

Polymers are classified according to the effect of temperature to:

1.3.2.1 Thermoplastic polymers

The characteristics of these polymers change with the influence of temperature. When the temperature rises, it becomes elastic and sticky. These polymers recover to their original solid state when the temperature is lowered. This is due to the fact that the molecules of a thermoplastic polymer are held together by relatively weak intermolecular forces (Vander Vales forces). Polyethylene, poly vinyl alcohol, Polyacrylamide , and polypropylene are examples of molecules that can slide over each other when heated [12], as shown in figure (1.2).

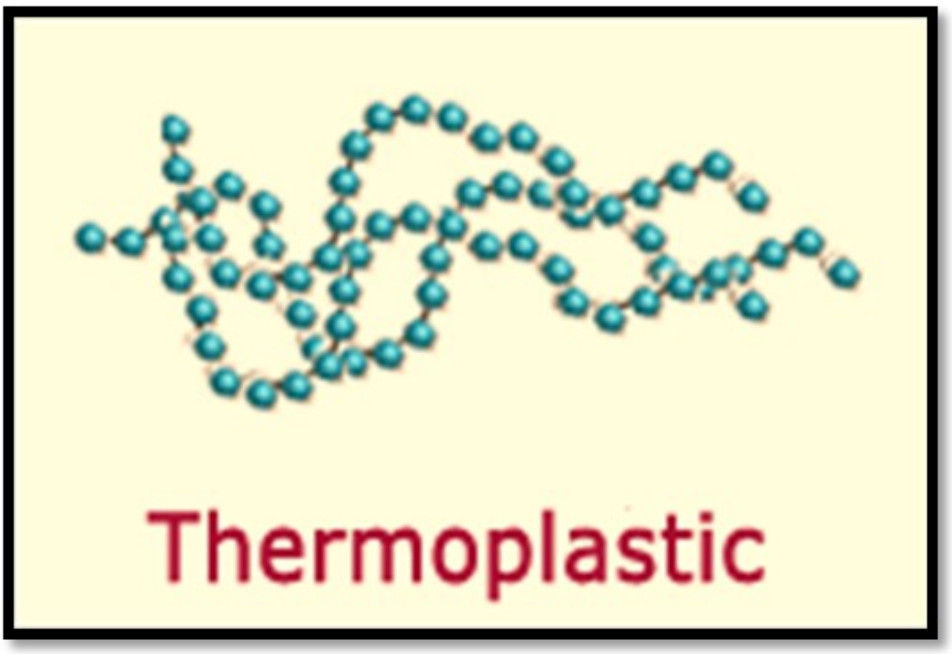

Figure (1.2): Atomic configuration of thermoplastic polymers [12].

1.3.2.2 Thermoset polymers

Some polymers undergo certain chemical changes on heating and convert themselves into an infusible mass. The curing or setting process involves chemical reaction leading to further growth and cross linking of the polymer

chain molecules and producing giant molecules. For example, resins, Phenolic, epoxy resins, urea , diene rubbers, etc. [13], as shown in figure (1.3).

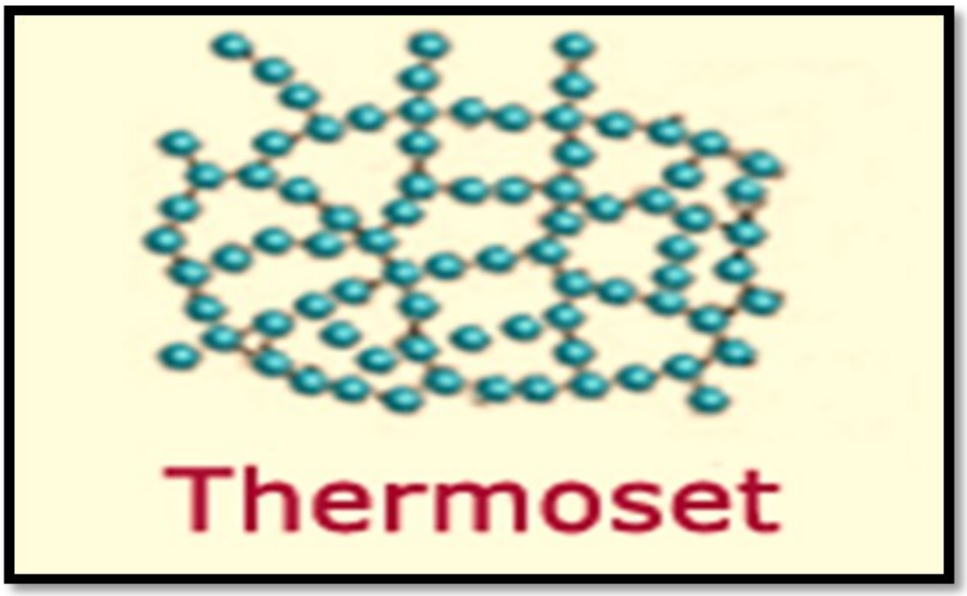

Figure (1.3): Atomic configuration of thermoset polymers [12].

1.4 Nanocomposites

Nanocomposites consist of polymers that may be natural or synthetic synthetic, and they are nanomaterials, which refer to materials with nano-sized topography or composed of nano-sized building components[13]. Although the terms nanomaterials and nanocomposite represent new and exciting areas in materials science, they have been used for centuries when they exist in nature. However, methods for characterizing and controlling the structure at the nanoscale have only stimulated much later[14].A nanocomposite, is a conventional compound consisting of two parts, a filler and a matrix. In a conventional composite usually a fiber such as glass fiber or carbon fiber is used as a filler, in a nanocomposite, the filler is a nanomaterial. Examples of nanomaterials are carbon nanotubes, carbon fiber tubs, and nanoparticles such as gold, diamond, silver, silicon and copper[15].The dispersion of inorganic nanocomposites into an organic polymer to form polymer nanocomposites has gained increasing attention in recent years. The fundamental and important role

that nanostructure control composition and morphology play in their applications, The new properties of nanocomposites can be obtained through the successful transfer of the properties of the original components into a single materials [16].An important and significant challenge in developing nanocomposites is to find ways to create macroscopic components that take advantage of the unique physical and mechanical properties of the very small objects within them. On the other hand, the fracture toughness of such biocomposites depends on the ultimate tensile strength(T) of the reinforcement. Crucially the use of nanomaterials allows the maximum theoretical strength of the material to be reached, because the mechanical properties become increasingly insensitive to defects at the nanoscale [17]. Electrical, thermal and electronic properties and the electrochemical properties of nanocomposites can differ significantly from those of their constituent [18]. The basic theory of nanocomposites is based on the principle that there is a very wide interface between the nano-sized building blocks and the polymer matrix that our study is based on this method or the nanocomposite [19].

1.5 Applications of Polymer Nanocomposites

The applications of polymer nanocomposites are based on: the matrix and the nanocomposites[20]. Among its many applications are:

1- Cars (gasoline tanks, fenders, interior and exterior panels...etc)

Construction (pull out the shape, panels) etc.

2- Electronics and electricity (printed circuits and electrical components) etc.
3- Cosmetics (controlled release of active ingredients) etc.
4- Dentistry (filling materials) etc.
5- Environment (biodegradable materials) etc.
6- Gas barrier (tennis balls, food and beverage packaging) etc.
7- Flame retardants, military, aerospace and commercial applications.

It can be noted that there are many industrial and medical applications of nanomaterials related to many fields, including engineering, biology, chemistry, computing, materials science, military applications, and communications, but their effects are difficult to enumerate Benefits of nanotechnology include improved manufacturing methods, water purification systems, improved food production methods and energy networks, physical health promotion, nanomedicine [21].

1.6 Materials Used in the Study

1.6.1 Polyvinyl alcohol (PVA)

PVA (Poly-vinyl alcohol) is synthetic polymer employed since the early 1930s in a wide range of industrial, commercial, medical and food applications including resins , surgical threads, lacquers and food-contact applications [22]. Poly (vinyl alcohol) is a synthetic polymer that comes in the form of a granular powder that is odorless, transparent, tasteless, white, or cream-colored [23]. Polycarbonate (vinyl alcohol), which may be combined in water, has the benefit of being resistant to solvents and oils, as well as having outstanding characteristics [24]. PVA fiber has high tensile and compressive strengths, tensile modulus, and abrasion resistance due to its highest crystalline lattice modulus. Many researchers have looked at using PVA as a filler or in cross-linked products, additionally, it has been widely employed as a thermoplastic polymer to make nontoxic, harmless, and living tissues, among other things [25,26]. It has been used in a wide range of applications and is also widely used in semiconductor applications [27]. Figure (1.4) shows the chemical structure of PVA.

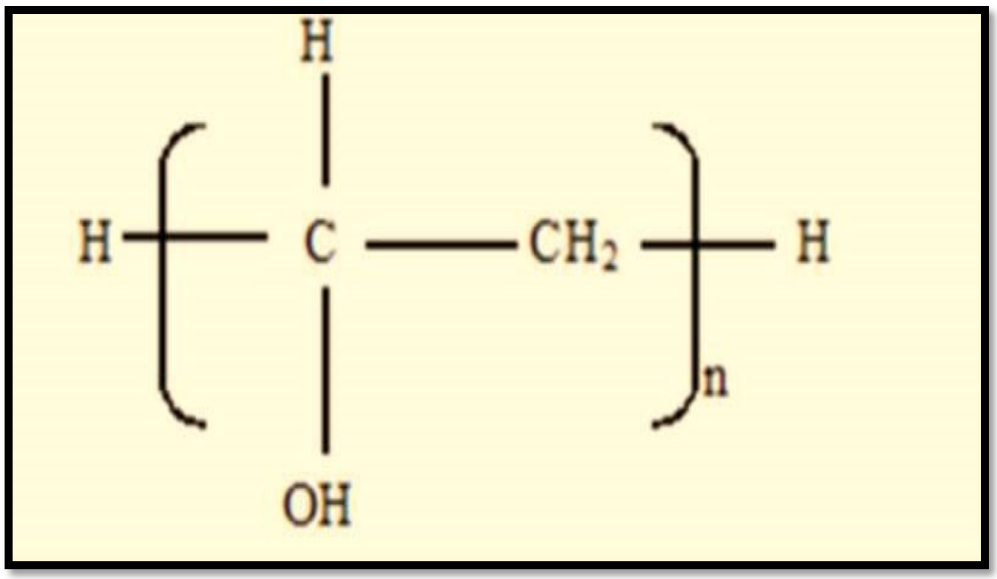

Figure (1.4) The Chemical Structure of PVA [27].

Table (1.1): Physical and Chemical Properties of (Poly vinyl Alcohol) (PVA) [28-34].

Property	Description
Appearance	White to an ivory white granular powder
Molecular formula	$(C_2H_4O)_n$
Solution PH	5- 6.5
Density	1.19 g/cm^3
Refractive index	1.47
Glass transition temperature T_g °C	85 °C
Melting temperature T_m °	228 °C
Boiling point	230°C
Solubility in water	soluble

1.6.2 Yttrium Oxide (Y_2O_3) Nanomaterials

yttrium oxide (Y_2O_3), an inorganic nanoparticle which is one kind of precious rare earth element. Recently, a geological survey of the United States. has emphasized that the estimated yttrium was 0.12% among rare earth elements, and demonstrated the end-use of Y_2O_3 in ceramic, metallurgy and phosphors. The leading countries of yttrium reserves include Australia, Canada, China, and India. Y_2O_3 is used as a component in uranium-resistant refractory ceramic, liquid reactive molten alloys and salts within the frame of atomic reactors [35], and it makes a superb defensive coating, as well as another suitable choice for silicon dioxide in metal-oxide-semiconductor devices. It is widely used in the ceramic field as abrasives and seals with high-temperature tolerability. It is also used in jet engine coating and used as an oxygen sensor in automobiles, It is corrosion-resistant to cutting tools [36]. In metallurgy, it is used as a grain-refining additive and deoxidizer, as a superior temperature conductor, and as the best alloys. The yttrium derivatives were used in electronic applications of microwave radar, digital communications, temperature sensors, nonlinear optics, photochemistry, and photoluminescence. Yttrium has played a vital part in yttrium aluminum garnet laser crystals that are applied in surgical procedures in medical and dentistry [37,38]. Table (1-2) explains some physical properties of Y_2O_3 [39-41].

Table (1-2)The physical properties of Y_2O_3[39-41].

Property	Description
Chemical formula	**Y_2O_3**
Molar mass	**225.81 g/mol**
Appearance	**White solid.**
Density	**5.010 g/cm^3, solid**
Melting point	**2425 °C**
Boiling point	**4300 °C**
Solubility in water	**insoluble**
Solubility in alcohol acid	**soluble**

1.7 Literature Review

In (2015) S. Sugumaran, *et. al,*[42], studied the characterization of the (PVA-Al_2O_3) composite thin films prepared by the casting method. They found that dependence of temperature and frequency for dielectric properties. The results also showed the study of insulating properties. The results indicated a higher refractive index, dielectric constant and lower dielectric loss for (PVA-Al_2O_3).

In(2016)J. J. Mathen, *et al,* [43], studied the improve of the optical and dielectric properties of PVA matrix with nano-ZnSe. The results showed that the dielectric constant and loss dielectric increase with increasing of ZnSe nanoparticles concentration. The optical conductivity increases with increasing the nanoparticles concentration.

In (2017) Majeed Ali Habeeb *et. al.* [44], studied the structural, optical and D.C Electrical Properties of (PVA/PVP/Y_2O_3) films via solution casting method and their application for humidity sensor. from optical microscope images obtained the Y_2O_3 form a continuous network inside the polymers when the proportion of (12 wt%). FTIR spectra shows shift in peak position as well as change in shape. Scanning electron microscopy (SEM) shows the surface morphology of the (PVA/PVP/Y_2O_3*)* films many aggregates or chunks randomly distributed on the top surface, homogeneous and coherent. The absorbance increases with increase the weight percentages of Y_2O_3. The energy band gap decreases with increasing the weight percentages of Y_2O_3. The D.C electrical conductivity increase by increasing yttrium oxide concentrations and temperature. The activation energy decreases by increasing Y_2O_3 concentrations. The resistance of the sensor decreased as humidity increased.

In (2018) B. Gurswamy, *et al* [45], studied the doping of Tin Oxide (SnO_2) nanoparticles on the structural and optical properties of the polymer blend (PVA/PVP). Membranes of the nanocomposites (PVA/PVP/SnO_2) nanocomposites were prepared using the solution casting technique. FTIR showed that SnO_2 nanoparticles react with the (OH) group of (PVA) and the carboxyl group (PVP) to form the compound within the mixing matrix. The optical study showed increased absorption in the UV region and transparency in the visible region.

In (2019) A. Hashim, *et. al* [46], studied structural and optical properties for nanocomposites of (PVA/PEO/CuO) nanocomposites. The optical microscope (OM) and optical properties were examined. They found when increasing the concentrations of CuO nanoparticles, the nanoparticles form a paths network inside the (PVA/PEO) blend. From optical properties, the absorbance of (PVA/PEO) blend increases with increase in CuO nanoparticles concentrations

which may be used for solar cell, transistors, diodes and other electronic applications. The optical constants increase while the transmittance and energy gap decrease as CuO nanoparticles concentrations increase. The results of application showed that the (PVA/PEO/CuO) nanocomposites with different CuO nanoparticles concentrations have high sensitivity for relative humidity which may be used as sensors for different humidity ranges.

In (2020) Q. Jebur, *et al.* [47], studied the dielectric and optical properties of (PVA/PEO/Fe_2O_3) nanocomposites. The results showed that the dielectric constant and dielectric loss are decreased while the electrical conductivity increases with the increase in frequency of applied electric field. The absorbance of (PVA/PEO/Fe_2O_3) nanocomposites improved as concentrations of iron oxide nanoparticles increased.

In (2021) Alrowaili, Z. A, *et al* ,[48], studied the structural and optical parameters of PVA/Y_2O_3 Polymer Nanocomposite Films. From the XRD analysis, it is found that the films are semi-crystalline and Y_2O_3 nanoparticles have cubic crystal structure. The average crystal size was 25 nm. FTIR spectra of all nanocomposite films exhibited good interaction between nano-Y_2O_3 and the PVA network. The morphological images obtained from SEM microscopy indicated good distribution of nano-Y_2O_3. Optical absorption spectra of the films enhanced with the incorporation of Y_2O_3. As the percentage of Y_2O_3 added increased, the direct optical energy gap, decreased from 5.42 to 5.31 eV.

In (2022) A. Nain, *et. al* [49], studied the effect of concentration of silver nanoparticles (Ag NPs) and ultraviolet (UV) irradiation on optical and structural properties of PVA/Ag nanocomposites. The structural and optical properties were examined. FTIR spectra show the interaction between PVA and Ag NPs and show changes caused in the structure of nanocomposite as the time of UV exposure increases. The presence of an absorption peak at around 410 nm recorded by UV-Vis spectrophotometer shows silver nanoparticles are formed. The absorption spectra increase with an increase in the concentration of Ag NPs

and with the increase in time of ultraviolet (UV) irradiation. The optical band gap decreased with an increase in the concentration of Ag NPs and with the increase in time of ultraviolet (UV) irradiation.

1.8 The Aims of the Study

Studying the effect of the Y_2O_3 nanoparticle on the structural, optical, and A.C electrical properties of PVA.

Chapter Two

Theoretical Part

2.1 Introduction

This chapter explains the main properties which make PVA/Y_2O_3 nanocomposite a good candidate for certain application. The study of structural and morphological properties was performed with optical microscope (OM), Fourier transform infrared (FTIR) spectroscopy, optical microscope, Optical properties of nanocomposite were performed with (absorbance, transmittances, electronic transitions and optical constants) and AC electrical properties were performed.

2.2 Morphological and Structural Properties:

2.2.1 Optical Microscope

Optical Microscope is a type of microscope that uses visible light and a system of lenses to magnify images of small samples. Optical microscopes are the oldest design of microscope and were possibly designed in their present compound form in the 17th century. Basic optical microscopes can be very simple, although there are many complex designs that aim to improve resolution and sample contrast. Historically, optical microscopes were easy to develop and are popular because they use visible light, so samples may be directly observed by the eye [50]. Optical microscopes are designed to create magnified visual or photographic images of small objects (Fig.2.1). To accomplish this, the microscope is designed to perform three tasks: create a magnified image of the sample, distinguish different details of the image, and make the final image visible to the human eye or camera. This class of characterization instruments includes everything from a simple magnifying glass to advanced multi-lens microscopes [51].

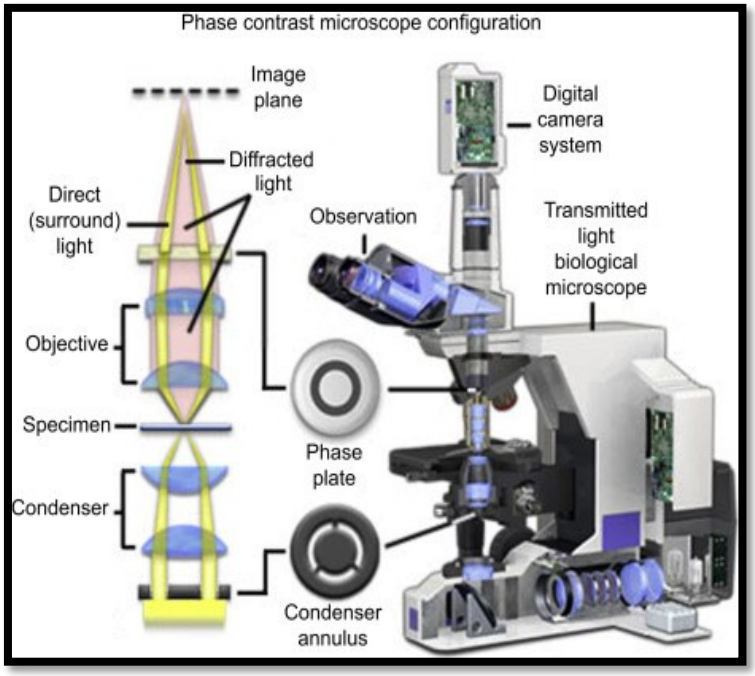

Fig (2.1): Optical Microscope [51].

2.2.2 Fourier transform infrared spectrometer (FTIR)

Fourier-transform infrared spectroscope (FTIR) is a technique used to obtain an infrared spectrum of absorption or emission of a solid, liquid or gas. An FTIR spectrometer simultaneously collects high-spectral-resolution data over a wide spectral range (Fig.2.2). This confers a significant advantage over a dispersive spectrometer, which measures intensity over a narrow range of wavelengths at a time. The term Fourier-transform infrared spectroscopy originates from the fact that a Fourier transform (a mathematical process) is required to convert the raw data into the actual spectrum. The goal of any absorption spectroscopy (FTIR, ultraviolet-visible "UV-Vis" spectroscopy, etc.) is to measure how much light a sample absorbs at each wavelength [52].

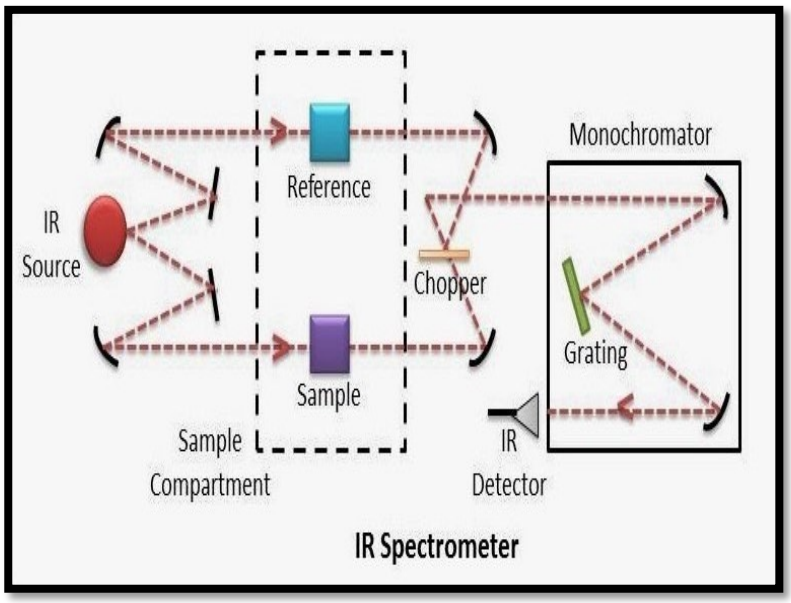

Fig (2-2): Fourier Transfer Infrared Spectroscopy (FTIR) [52].

2.3 Optical Properties

The study of the optical properties of polymers increases our knowledge of the type of polymer internal structure; nature of the bonds and expands the potential scope of polymer application, Knowing the spectrums of absorption and transmittance a polymer assists in identifying many optical properties in different ranges of wavelengths. Conducting examination at the ultraviolet spectrum range enables us to know the type of the bonds, orbital and energy beams. The study at the visible spectrum range provides sufficient information about the behavior of a matter to solar applications. The study at the infrared range is very important in knowing the general structure of a polymer and the elements consisting its chemical structure [53]. Knowing the spectrum of absorption and transmittance of a polymer assist in identifying many optical properties in different ranges of wavelengths. Conducting examination at the ultraviolet spectrum range enables us to know the type of the bonds, orbital and energy beams. Optical properties are commonly characterized using spectroscopic techniques including UV-visible and photoluminescence spectroscopy, which both yield information about the electronic structure of nanoparticles [54].

2.3.1 Light absorbance and electronics transitions

The total molecular energy has divided into the electronic energy (E_{ele}), vibration energy (E_{vib}), rotational energy (E_{rot}) and transitional energy (E_{trans}). The absorbance of electromagnetic wave results in a change in the total energy of the molecule due to the change in the different energies [55].

$$\Delta E_{total} = \Delta E_{ele} + \Delta E_{vib} + \Delta E_{rot} + + \Delta E_{trans} \quad \ldots\ldots\ldots\ldots\ldots\ldots\ldots\ldots\ldots\ldots (2\text{-}1)$$

It has been noted that the visible and ultraviolet spectrums are the spectrum of electronic absorbance; the remaining is the spectrum of other absorbance. The E_{ele} is the clearest in the absorbance spectrum. The reaction of the photon with the molecule makes the electrical field of the photon works in a manner that agitates the electronic structure of the molecule to the point that makes the photon disappear and its energy transferred to the molecule whose state has been changed to an excited state [56, 57].

2.3.2. Optical absorbance (A)

Absorbance can be defined as the ratio between absorbed light intensity (I_A) by material and the incident intensity of light (I_o) [58].

$$A = I_A \backslash I_O \quad \ldots\ldots\ldots\ldots\ldots\ldots\ldots\ldots\ldots\ldots\ldots\ldots\ldots\ldots\ldots\ldots (2\text{-}2)$$

2.3.3. Optical transmittance (T)

It is the ratio between the intensity of the beam from the film I_T to the intensity of the beam incident on the film thin I_O and expressed by the relationship [59].

$$T = I_T / I_o \quad \ldots\ldots\ldots\ldots\ldots\ldots\ldots\ldots\ldots\ldots\ldots\ldots\ldots\ldots\ldots\ldots (2\text{-}3)$$

2.3.4. Optical reflectance (R)

The absorbance (A) and transmittance (T) can also be calculated from the following equation [60]:

$$R + A + T = 1 \quad \text{.....(2-4)}$$

Where: R is reflectance, T is transmittance, and A is absorbance.

When the fall of the beam of monochromatic light perpendicular to the section of the surface of the samples the part of the beam will reflect and implement the remaining part. This force could face the process of absorption also in order to keep the algebraic sum of these parts equal to the value one.

2.3.5. Optical constants

There are many ways to find the optical constants of absorption coefficient, refractive index, extinction coefficient, the complex of dielectric constant (real and imaginary) and optical energy gap:

1. Absorption Coefficient (α)

The optical absorbance coefficient (α) of the film is calculated by the equation [61]:

$$\boldsymbol{\alpha} = 2.303A/d \quad \text{.....(2-5)}$$

Where (d) represent a thickness of sample.

2. Refractive Index (n)

It is the ratio of light speed in vacuum to its speed in a medium. This index shows how far a matter is affected by the electromagnetic waves. The refraction index consists of two parts: real and imaginary. It can be expressed by the following equation [62];

$$n = c/v \quad \ldots \text{(2-6)}$$

where (n) is the refraction index, (c) is the light speed in vacuum and (v) is the light speed in matter. Reflectance (R) can also be defined as the ration of the reflected ray relation at the borderline between two mediums to the incident ray. The relation between reflectivity and refractive index is shown in the following equation;

$$R = (n -1)^2 +k^2 /(n+1)^2 + k^2 \quad \ldots \text{(2-7)}$$

where (k) is the extinction coefficient.

The rate of absorption of light is directly proportional to the intensity of the incident light at a specific wavelength, and this physical phenomenon is common and lead to the decay of the light intensity exponential as it passes.

Refractive index can be expressed by the following equation [63];

$$n = \frac{1+ (R)^{\frac{1}{2}}}{1-(R)^{\frac{1}{2}}} \quad \ldots \text{(2-8)}$$

The reflectance of thin films was measured directly by using the Specular Reflectance Attachment (with 5° incident angle) of the UV-Vis-NIR double beam spectrophotometer (Shimadzu, UV-1800). The technique of specular reflectance is often applied to the examination of semiconductors, optical materials, multiple layers, etc. The 5° incident angle minimizes the influence of polarized light. Thus, no polarizer is needed to perform the reflectance measurements.

3. Extinction Coefficient (k)

The electrical coefficient the amount of photons absorbed by the membrane, that is, the energy absorbed by the electrons of the material, and expresses the following relationship [60]:

$$k = \alpha\lambda/4\pi \qquad \text{(2-9)}$$

Where (λ) is the wavelength of the incident ray and (α) absorption coefficient.

4. Complex Dielectric Constant

The matter of ability of polarization is represented the dielectric constant. The matter is reflected to various frequencies in a complex manner. at optical frequencies, it is characterized by the waves of the light, where the electronic polarity considered as dominating above all other remaining polarization types. and this polarization is called dielectric constant known as the following relationship [64]

$$\varepsilon = \varepsilon_1 - i\varepsilon_2 \qquad \text{(2-10)}$$

Where ε_1 the real part of the dielectric constant, ε_2 the imaginary part of the dielectric constant [64].

$$\varepsilon = N^2 \qquad \text{(2.11)}$$

$$(n - ik)^2 = \varepsilon_1 - i\varepsilon_2 \qquad \text{(2.12)}$$

From equation (2.10) real and imaginary complex dielectric coefficient can be written as follows [64]:

$$\varepsilon_1 = (n^2 - k^2) \qquad \text{(2.13)}$$

$$\varepsilon_2 = (2nk) \qquad \text{(2.14)}$$

The optical conductivity (σ_{op}) depends directly on the refractive index (n) and absorption coefficient (α) by the following relation [65]:

$$\sigma_{op} = \alpha nc/4\pi \qquad \text{(2.15)}$$

2.3.3 Fundamental absorption edge

The fundamental absorption edge can be defined as the rapid increasing in absorbance when absorbed energy radiation is almost equal to the band energy gap; therefore, the fundamental absorption edge represents the less difference in the energy between up point in valance band to bottom point in conduction band [66].

2.3.4 Absorption regions

Absorption regions can be classified to three regions [67]:

A) High absorption region

This region is shown in Figure (2.3). In part (A), the magnitude of absorption coefficient (α) is larger or equal to (10^4 cm^{-1}). From this region the magnitude of forbidden optical energy gap (Eg^{opt}) can be introduced.

B) Exponential region

This region is shown as in Figure (2.3). In part (B) the value of absorption coefficient (α) is equal to (1 cm^{-1} < α < 10^4 cm^{-1}). It refers to transition between the extended levels from the Valens band (V.B.) to the local level in the conductive band (C.B.) and vice versa, transited from local levels in (V.B.) to the extended levels in the bottom of conductive band (C.B.)

C) Low absorption region

The absorption coefficient (α) in this region is very small, it is about (α<1cm^{-1}). The transition happens in this region because of state density inside space motion resulted from faults structural [68], as in figure (2.3)

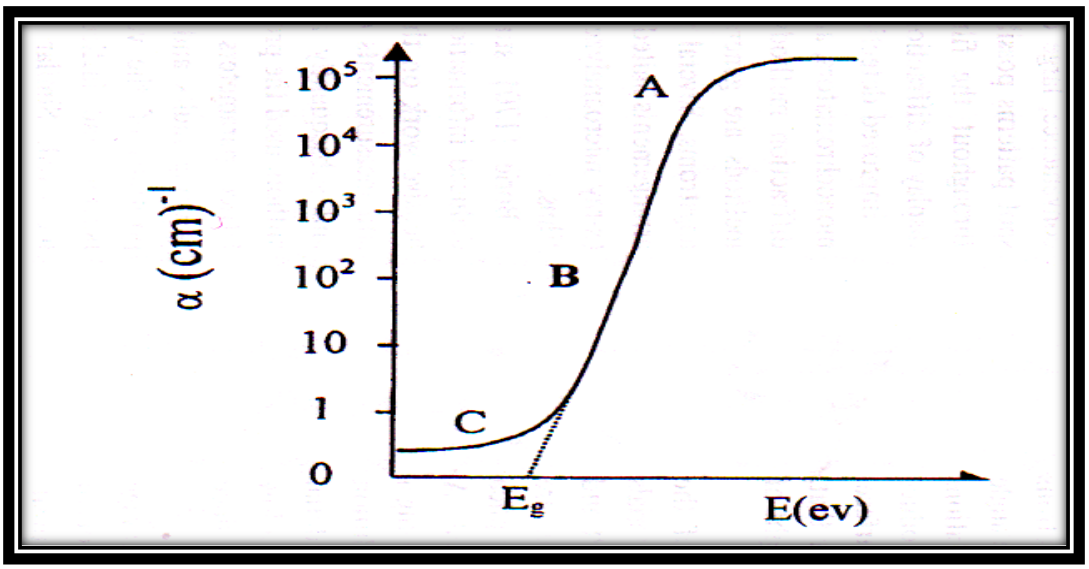

Fig (2.3):The variation of absorption edge with absorption regions [67].

2.3.5 The Electronic Transitions

Electronic transitions are divided into two types:

2.3.5.1 Direct transitions

Direct transitions occur when conduction band (C.B) and valance band at the same point in the space .This means that they have the same value of wave vector (ΔK=0). In this case the absorption will appear at (*Eg=hv).* This type occurs without a noticeable change in energy and momentum. There are two types of direct;

1. Allowed direct transition

Figure (2.4.a) shows that this transition happens from top points in the valence band (V.B) and the bottom point in the conduction band (C.B). The empirical relationship for this type of transition is given by the equation [69]:

$$\alpha h\nu \approx [h\nu - Eg]^{1/2} \quad \ldots\ldots\ldots\ldots\ldots\ldots\ldots\ldots\ldots\ldots\ldots\ldots \text{(2-16)}$$

Where (α) is the absorption coefficient, (h) Plank constant (6.625×10^{-34} $J.s$), (v) is the frequency in (Hz), (E_g) energy gap.

2. **Forbidden direct transitions**

Figure (2.4.b) Shows that this transition happens from near the top points of valence band (V.B) and the bottom points of conduction band (C.B). The empirical relationship which corresponds to this transition is given by the equation [70]:

$$\alpha h\nu \approx [h\nu - Eg]^{3/2} \quad \text{.....(2-17)}$$

2.3.5.2 Indirect transition

This transition happens when the bottom of conduction band (C.B) is not over the top of valence band (V.B), in curve (E-K) Fig (2.4). The electron transits from V.B are not perpendicularly, where the value of the wave vector of electron before and after transition is not equal ($\Delta k \neq 0$). This transition type happens with the help of a like particle called "Phonon". There are two types of indirect transitions, this type of transitions occurs by help phonon to conservation of movement resulted from variation in wave vector for the electron [71].

$$h\nu = E_g \pm E_p \quad \text{.....(2-18)}$$

where E_p is the energy of absorbed or emitted phonon.

1. Allowed indirect transitions

Figure (2.4.c), in the case of moving from the highest point of the valence band to the lowest point of the bottom of the conduction band, which are found in the difference region of K-space [71].

$$\alpha h\nu \approx [h\nu - Eg]^{2} \quad \text{.....(2-19)}$$

2 Forbidden indirect transitions

These transitions happen between near points in the top of (V.B.) and near points in the bottom of (C.B.) [72,73], as shown in fig.(2.4-d). The absorption coefficient for transition with a phonon absorption is given by [71]:

$$\alpha h\nu = B(h\nu - E_g^{opt} \pm E_{pn})^r \qquad \ldots\ldots\ldots\ldots\ldots\ldots\ldots\ldots\ldots\ldots(2\text{-}20)$$

Where: $E_{ph.}$: energy of phonon, is (-) when phonon absorption, and (+) when phonon emission.

(r = 2) for the allowed indirect transition.

(r = 3) for the forbidden indirect transition.

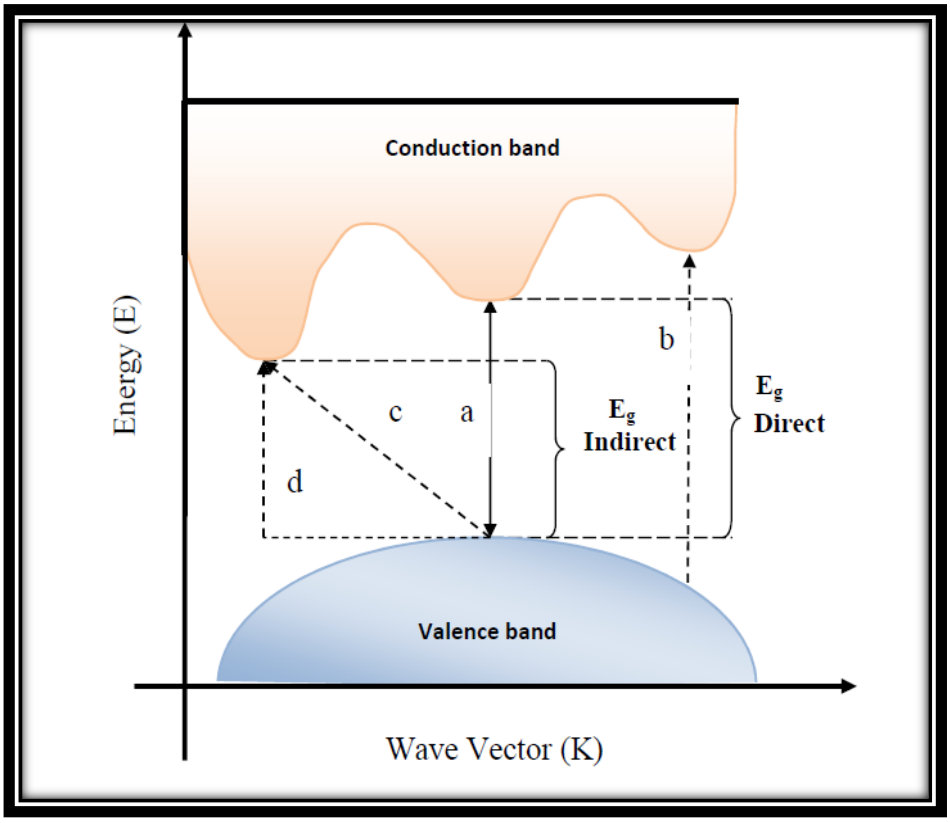

Fig. (2.4) The types of transition [71].

(a) allowed direct, (b) forbidden direct, (c) allowed indirect, and (d) forbidden indirect.

2.4. The A.C Electrical Conductivity

A.C conductivity affects the frequency of the electrical field [74]. Dielectric spectroscopy is based on the calculation of current and voltage phases and the amplitude A.C system. It is commonly used for the study of dielectric properties of polymers e.g. (ε', tanδ) [75]. The electrical conductivity of isolation polymer materials can be improved through adding certain conductive fillers [76]. The dielectric constant represents the ratio of the capacitance of the condenser that contains an insulator material between its conductive plates, to the capacity of the same size but with vacuum between its plates. Its value varies from material to material based on the amount of polarization that occurs in the material [77].

When an alternating potential $V = V_m e^{i\omega t}$ [77] is applied through a capacitor (C) loaded with an insulator, the current going through the capacitor will precede the potential by $\pi/2$ [78].

$$I = j\omega c v_m \qquad \text{.....} \quad (2.21)$$

Where (ω) is the applied angular frequency of the filed (ω=2πf), (j) refers to the number of imaginary and is equal to $\sqrt{-1}$, (C) is the capacitance of a capacitor, and (V_m) is the highest voltage. The angle between electric current and voltage is less than π/2, as seen in figure (2.5). The sum of the conduction current (I_p) is assumed to be electric current. This is in the same phase with voltage, whereas the capacitates current (I_q) is with the phase variation (π/2). The current can be obtained through the equation below[79]:

$$I = I_P + jI_q \qquad \text{.....} \quad (2.22)$$

The capacitance of a condenser consisting of two parallel plates can be defined through the following equation [80]:

$$C = \frac{A_r}{d} \varepsilon \varepsilon_o \qquad \text{.....} \quad (2.23)$$

where (A_r) is the area, and (d) is the thickness.

By substituting equation (2.24) in (2.22), the following relation is obtained:

$$I = i\,\omega\,\varepsilon\,\varepsilon_o V A_r/d \quad \text{………………………………… (2.24)}$$

The dielectric constant is then viewed as a complex quantity (ε). The difference of the real and imaginary components of the complex dielectric constant is defined as follows [81]:

$$\varepsilon = \varepsilon' - i\,\varepsilon'' \quad \text{………………………………………(2.25)}$$

where (ε'') is the dielectric loss.

$$I = i\,\omega\varepsilon_o \frac{A_r}{d} (\varepsilon' - i\,\varepsilon'')\, V \quad \text{…………………………………(2.26)}$$

By comparing equation (2.27) to (2.22), the following can be obtained:

$$I_p = \omega\varepsilon_o\,\varepsilon'' \frac{A_r}{d} V \quad \text{………………………………………(2.27)}$$

$$I_q = \omega\varepsilon_o\,\varepsilon' \frac{A_r}{d} V \quad \text{………………………………………(2.28)}$$

Figure (2.6) shows that the loss factor (tanδ) is calculated by the following equation [79]:

$$\tan\delta = I_p / I_q = \varepsilon''/\,\varepsilon \quad \text{………………………………………..(2.29)}$$

The capacitor can be represented by an ideal capacitor connected in parallel with a resistance R_P at low frequencies, so:

$$I = I_p + iI_q = \frac{V}{R_P} + i\,\omega C_p V \quad \text{…………………………………….(2.30)}$$

Hence, the impedance **z** is then given by

$$\frac{1}{Z} = \frac{1}{R_P} + i\,\omega\,C_p \quad \text{……………………………………(2.31)}$$

From equations (2.28), (2.29) and (2.31), one can write [78]:

$$R_P = d / \omega A_r \varepsilon_o\,\varepsilon'' \quad \text{…………………………………(2.32)}$$

$$\varepsilon'' = 1 / \omega R_P C_o \quad \text{…………………………………(2.33)}$$

$$C_P = \varepsilon_o\,\varepsilon' A_r /d \quad \text{…………………………………(2.34)}$$

$$\varepsilon' = C_P / C_o \quad \text{…………………………………(2.35)}$$

where Cp is the capacitor containing an insulator materials, Co is the capacitor containing vacuum.

The dissipated power in the insulator is represented by the existence of alternating potential as a function of the alternating conductivity, as explained in the following equation:

$$\sigma_{A.C} = \omega \, \varepsilon_o \, \varepsilon'' \qquad \text{......................................} \ (2.36)$$

$\sigma_{A.C}$ represents the measu rement of the temperature produced by the insulation material arising from the vibration of the charges or rotation of the dipoles in their positions. This is the result of the alternation of the field [82].

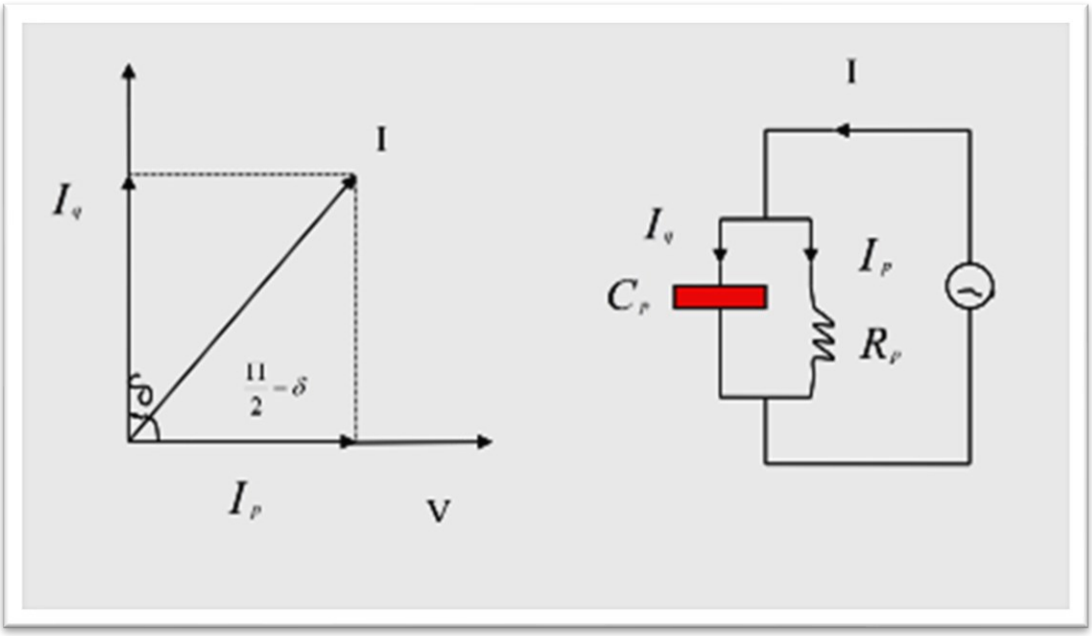

Figure (2.5) The circuit equivalent to non-ideal capacitor [79].

Chapter Three

Experimental Work

3.1. Introduction

In any experimental work, there are a specific mechanism for manner of working, devices to examine the samples and an exact theorems to explain the results . In this chapter illustrate in details the materials used and the preparation process with devices that used in this work to find out the structural, optical, and electrical properties.

3.2. The Utilized Materials

3.2.1. Matrix material

3.2.1.1. Polyvinyl Alcohol (PVA)

PVA as used in this study having average molecular weight of (12000-18000g /mol), its physical form: pure, solid, white, odourless granules. CAS Number:9002-89-5, its melting point of PVA is 228^0C.

3.2.1.2. Additive Material

Yttrium Oxide (Y_2O_3) nanoparticles were used in the study having purity: 99.8%, form: powder, white in colour, density: 5.01g/cm^3, average grain size:50 nm, made in China by Honqwu international.

3.3. The Preparation of (PVA/Y_2O_3) nanocomposites

The (PVA/Y_2O_3) nanocomposites are prepared by dissolving(1g) from PVA polymer in (50) mL of distilled water separated uneven concentrations.

At temperature (70ºC), the polymer PVA were mixed by using with magnetic stirrer to mix these polymers for a period exceeding one hours in order to obtain a more homogeneous solution and (Y_2O_3) was added to the solvent of polymer with various weight ratios (0, 1.5, 3, 4.5 and 6 wt.%) as shown in tables (3-1).

This combination was cast in a template (Petri dish) at a drop height of 10 cm and a thickness of (0.21-0.23) mm, and dried for seven days using the casting method. Finally, the samples are ready for the structural, optical and electrical as shown in figure (3.1)

Table (3-1): Weight percentages for nanocomposites (PVA/Y_2O_3)

PVA wt.%	Y_2O_3 wt.%
100	0
98.5	1.5
97	3
95.5	4.5
94	6

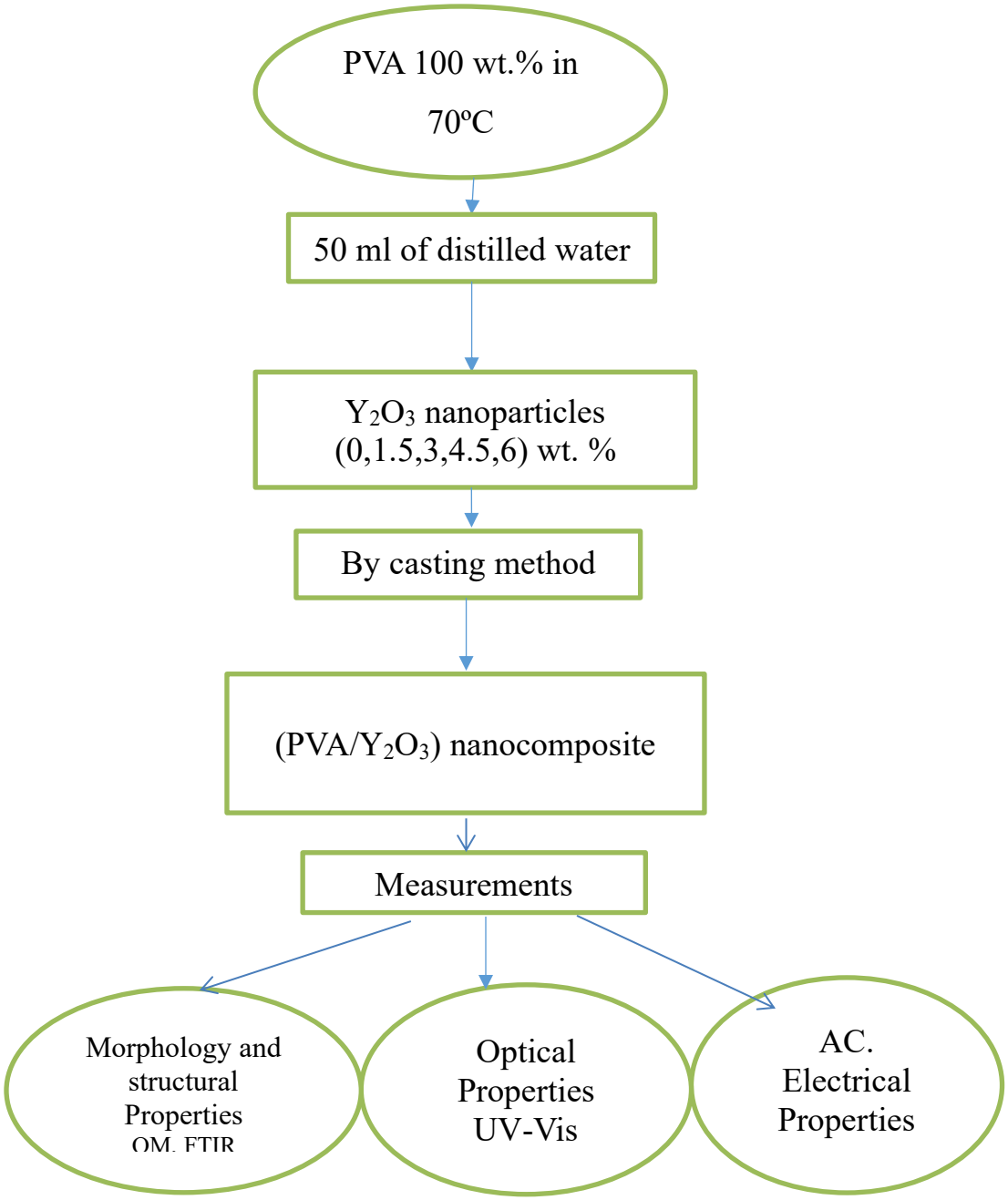

Figure (3.1): Scheme of Experimental work.

3.4 Measurement of Structural Properties for (PVA/Y_2O_3) Nanocomposites

3.4.1 Optical Microscope (OM)

Olympus (Top View) type Nikon-73346 optical microscope with automatic camera controlled by light intensity investigated the (PVA/Y_2O_3) nanocomposites specimens. The work on this device was carried out in University of Babylon College of Education for pure science, this measurement under magnification (40x), as shown in Figure (3.2).

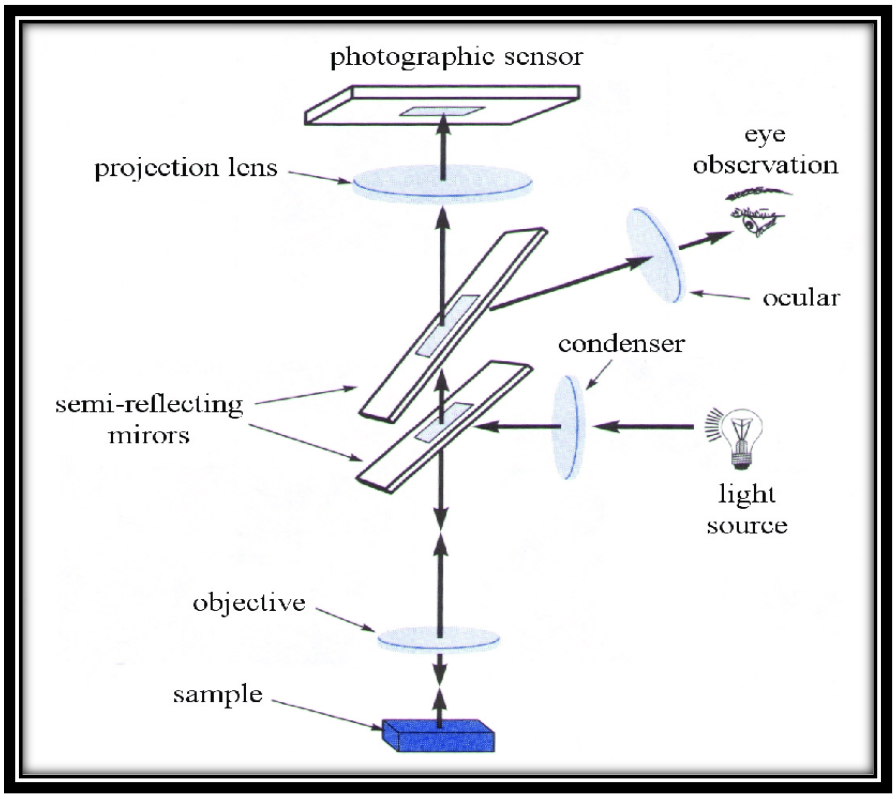

Figure (3.2): The Diagram for Optical Microscope.

3.4.2 Fourier Transformation Infrared (FTIR) Spectroscopy

Fourier Transformation Infrared (FTIR) Spectroscopy was used to capture spectra (Bruker company, German origin, type vertex -70), operated with wavenumber (400-1000) cm^{-1}. In the University of Babylon College of Education for Pure Sciences-Department of Physics, FTIR was adopted, as shown in Figure (3.3)

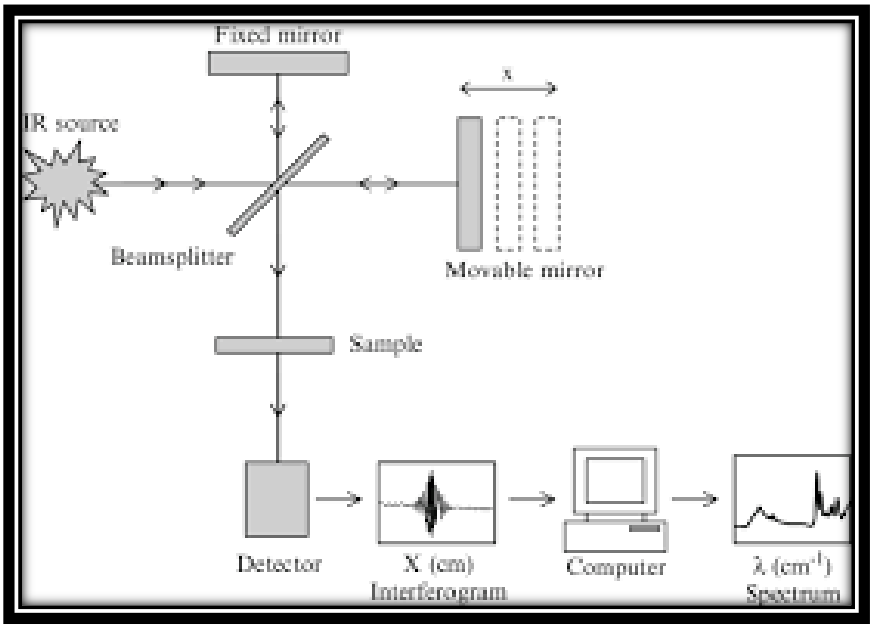

Figure (3.3): FTIR Diagram Spectroscopy.

3.5 Optical Properties Measurements

Measurements were made with a Shimadzu UV-18000A double beam optical spectrophotometer (200-1100nm) on films made of (PVA/Y_2O_3) nanocomposites. The University of Babylon College of Education for Pure Sciences implemented this measurement as indicated in Figure (3.4).

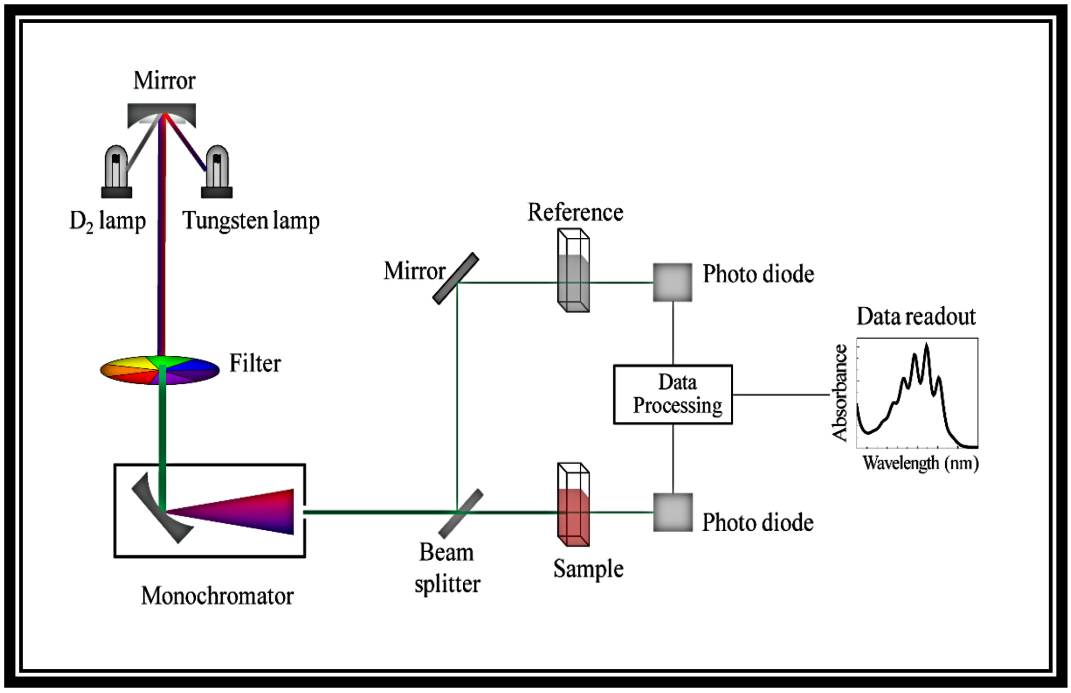

Figure (3.4): The Diagram for UV–Visible Spectrophotometer (Shimadzu-1800).

3.6. Measurement of A.C. Electrical Conductivity

Alternative current (A. C.) Electrical Conductivity was calculated by (L.C.R) kind HIOKI 3532-50 LCR Hi TESTER (Japan) at laboratories of the University of Babylon /College of Education for Pure Sciences. Figure (3.5) displays a picture the system of A .C electrical measurement dispersion factor and capacitance were reported for all samples at a frequency between (100-5×10^6) Hz at room temperature. Dielectric constant, dielectric loss, and conductivity have been calculated from this data.

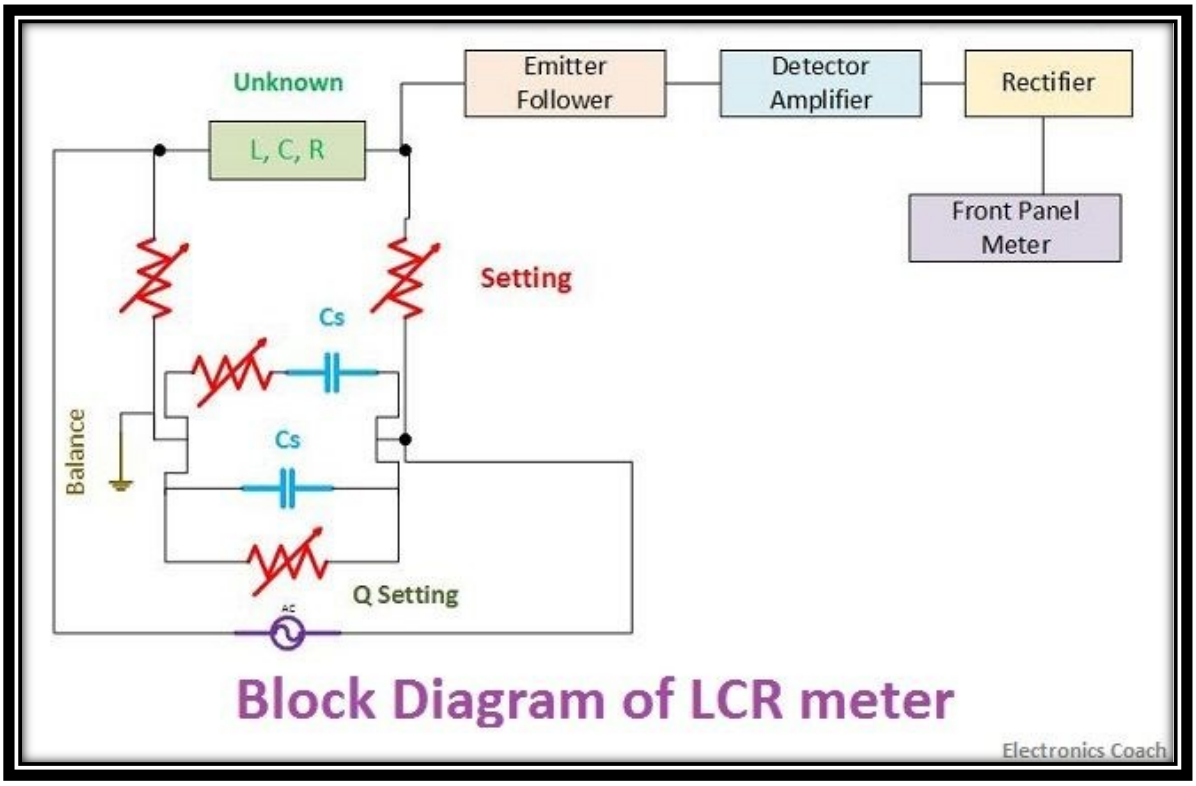

Figure (3.5): LCR Diagram Hi TESTER Devices

Chapter Four

Results, Discussions and Future Works

4.1 Intorduction

This chapter includes the findings as well as a review of the systemic, optical and (A.C) electrical. It will also discuss the effect of different concentrations additive nanoparticles (Y_2O_3) in the optical microscope, Fourier transform infrared ray (FTIR).

4.2 The Morphological and Structural Properties.

4.2.1 The Optical Microscope

The optical microscope (OM) images of pure PVA and (PVA-Y_2O_3) nanocomposites with different concentration (0,1.5,3,4.5 and 6) wt.% of Y_2O_3 nanoparticles are shown in figure (4.1) with different concentrations of Y_2O_3 nanoparticles at magnification power (x10). There are a lot of differences between pure sample and other nanocomposites with adding various concentrations of Y_2O_3 nanoparticles however, figures demonstrate the addition of Y_2O_3 distributed throughout the polymer matrix with homogenous and ordered shape as well as the apparent of Y_2O_3 network within the polymer matrix. With increasing concentration at 6 wt.%, lead to formation path inside the polymer matrix. These results are agreed with [80].

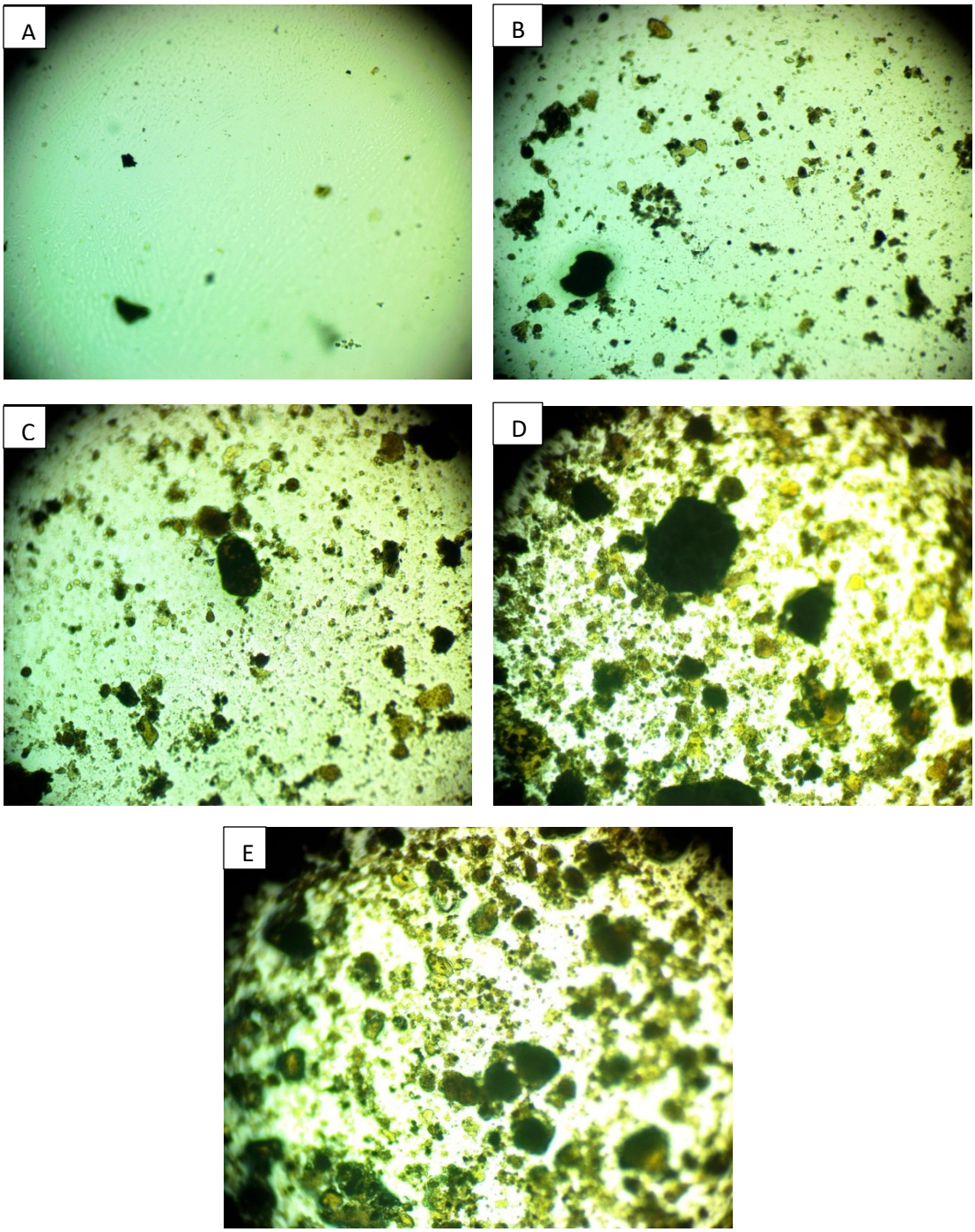

Figure (4.1): Photomicrographs (x10) for PVA/Y_2O_3 nanocomposites A. PVA, B. 1.5 wt.% Y_2O_3, C. 3wt.% Y_2O_3, D. 4.5wt.% Y_2O_3 and E. 6wt.% Y_2O_3

4.2.2 Fourier Transform Infrared Ray (FTIR)

The FTIR spectra of pure PVA and (PVA/Y_2O_3) nanocomposites with different concentrations of Y_2O_3 nanoparticles were recorded at room temperature in the range (400-4000) cm^{-1} are shown in Figure (4-2). At this figures in image (A), FTIR spectrum of pure PVA is corresponding to the broadness stretching vibrations of O–H, CH_2 stretching in an asymmetrical direction and medial alkyne C=N stretching vibration occurs at 3259.19 cm^{-1}, 2906.49 cm^{-1} and 1326.67 cm^{-1}, respectively, in agreement with researchers [81]. The absorption peak at 1085.15 cm^{-1} corresponds to the C–O stretch for secondary alcohol were observed in PVA hydrogels. Bending of C-H (832.90) cm^{-1} CO is an abbreviation for symmetric stretching [82,83]. The IR spectra of PVA/Y_2O_3 in images (B to E) contains all the characteristic peaks of PVA and the added NPs, it can be noticed that there are slightly shifted toward higher wavenumbers, as a result of the addition of different wt.% of Y_2O_3 NPs. Clearly from the nanocomposites spectra there no interactions between polymer matrix and NPs

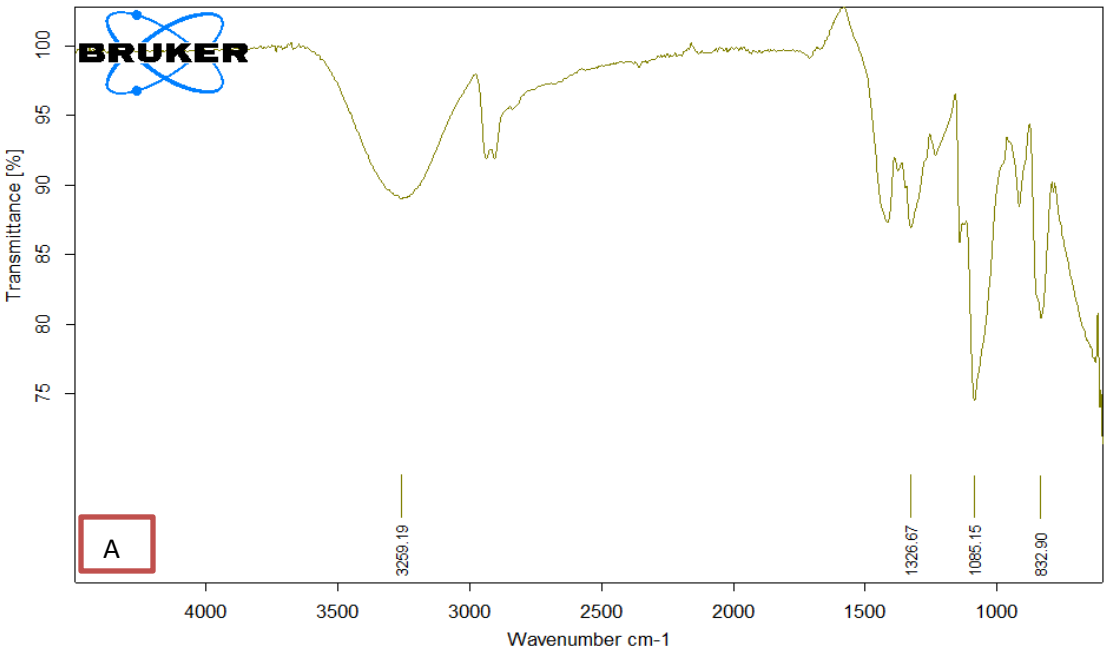
BRUKER
Transmittance [%]
100
95
90
85
80
75
A
3259.19
1326.67
1085.15
832.90
4000
3500
3000
2500
2000
1500
1000
Wavenumber cm-1

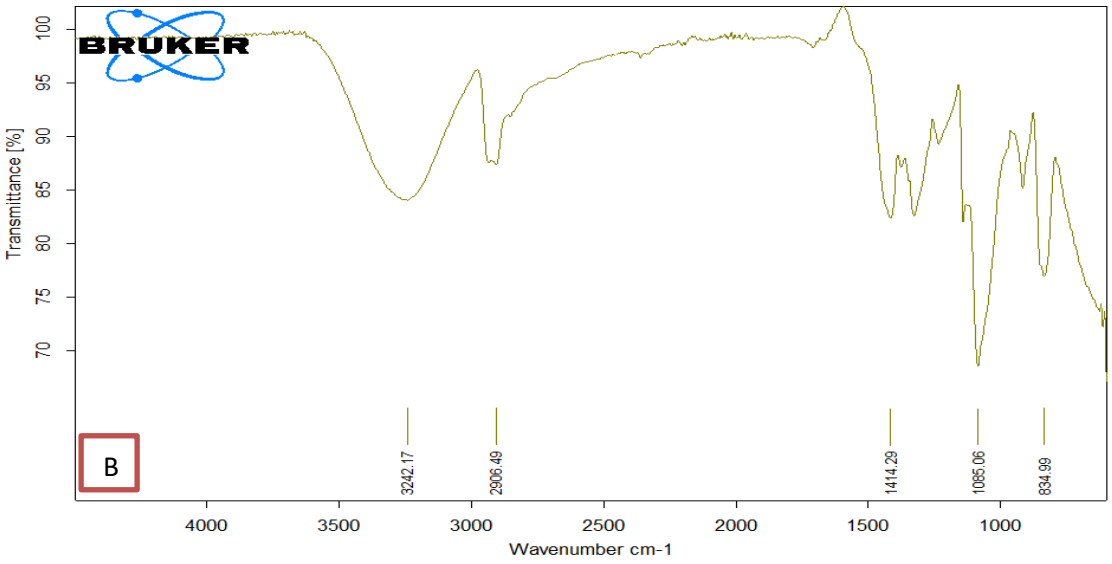
BRUKER
Transmittance [%]
100
95
90
85
80
75
70
B
3242.17
2906.49
1414.29
1085.06
834.99
4000
3500
3000
2500
2000
1500
1000
Wavenumber cm-1

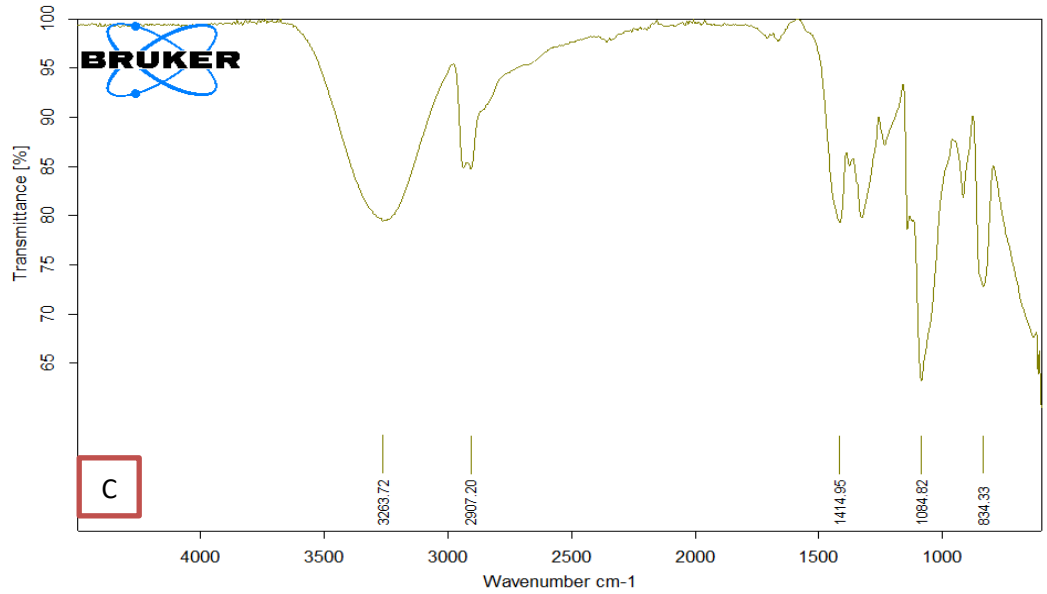
BRUKER
Transmittance [%]
100
95
90
85
80
75
70
65
C
3263.72
2907.20
1414.95
1084.82
834.33
4000
3500
3000
2500
2000
1500
1000
Wavenumber cm-1

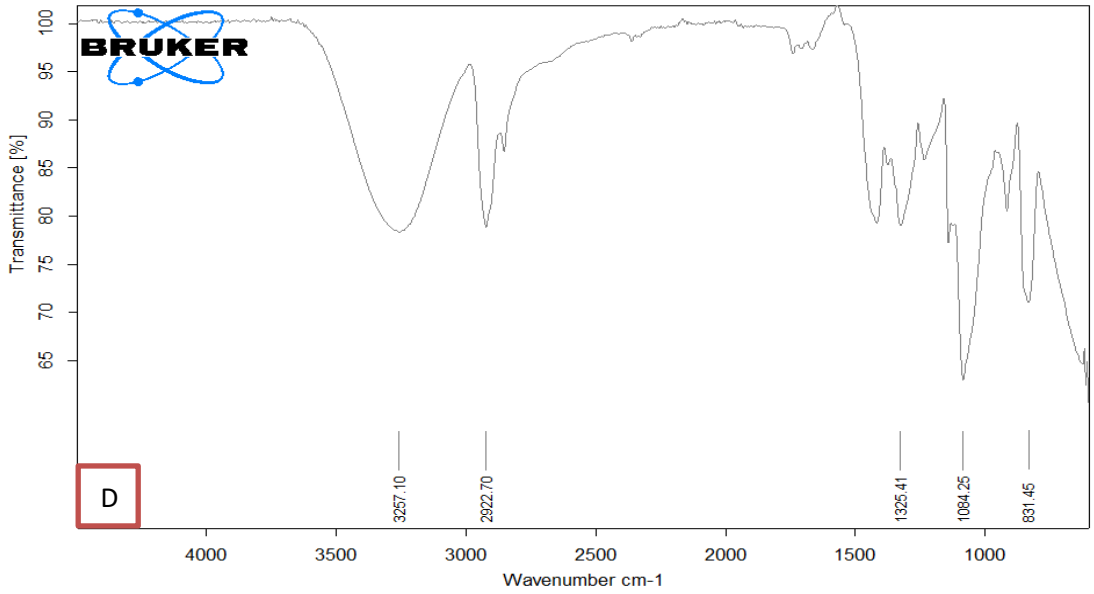
BRUKER
Transmittance [%]
100
95
90
85
80
75
70
65
D
3257.10
2922.70
1325.41
1084.25
831.45
4000
3500
3000
2500
2000
1500
1000
Wavenumber cm-1

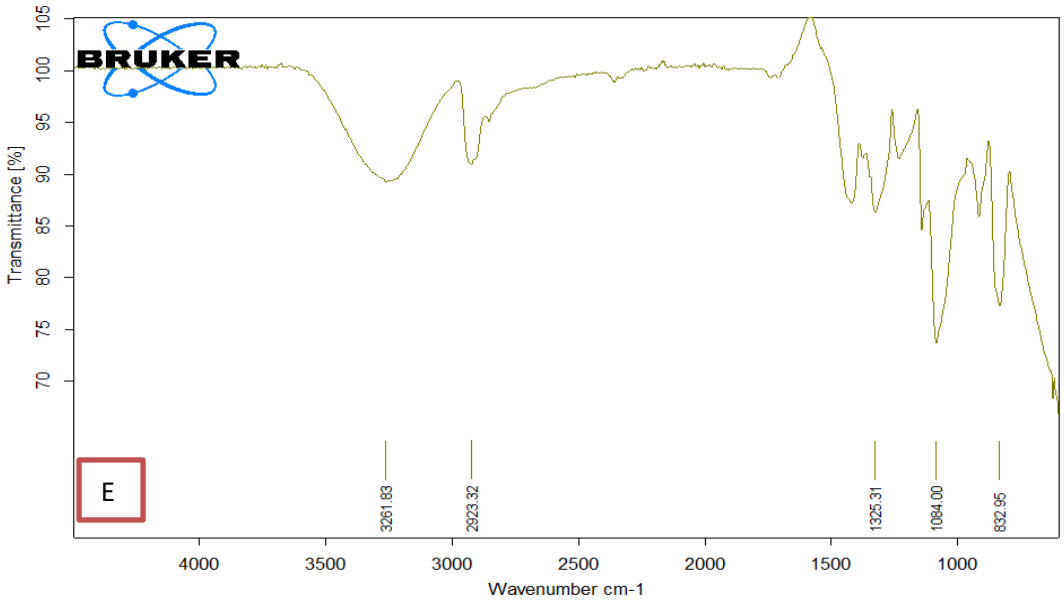

Figure (4.2). FTIR spectra For (PVA-Y_2O_3) Nanocomposites: (A) For (PVA), (B) For1.5wt% (C) For 3 wt%, (D) For 4.5 wt% ,(E) For 6wt%.

4.3 The Optical Properties

The main purpose of studying the optical properties of the (PVA/Y_2O_3) nanocomposites is to identify the effect of adding the Y_2O_3 nanoparticles on the optical properties of PVA. The study involves measuring the absorbance spectrum of (PVA/Y_2O_3) films at room temperature, determining the absorption, extinction, and other optical constants, defining the forms of electronic transitions, and measuring energy gaps.

4.3.1 The Absorbance and Transmittance of (PVA-Y_2O_3) Nanocomposites

Figure (4.3) shows the variation of absorbance for (PVA/Y_2O_3) nanocomposites with different concentration of Y_2O_3 wt.% nanoparticles versus wavelength of the incident light. The figure shows increasing of the absorption for the samples of (PVA/Y_2O_3) nanocomposites at (UV region) with increasing of the concentrations for (Y_2O_3) nanoparticles, this is due to the excitations of

donor level electrons to the conduction band at these energies. The high absorbance of samples for nanocomposites (PVA/Y_2O_3) at UV region attributed to the energy of photon enough to interact with atoms; the electron excites from a lower to higher energy level by absorbing a photon of known energy. This behavior agree with the results of researchers[84]. At visible and near infrared regions, the absorbance of all samples for nanocomposites has low values, this behavior attributed to the energy of incident photons doesn't enough energy to interact with atoms, thus the photons will be transmitted when the wavelength increases[85]. Figure (4.4) shows that the variation of the transmittance of (PVA/Y_2O_3) nanocomposites with wavelength of the incident light. As shown in figure, the absorbance increases and the transmittance decreases with the increasing of the concentrations for (Y_2O_3) nanoparticles, this is due to the agglomeration of nanoparticles with increasing concentration and increase of the number of charge carriers[86]. The decreased in transmittance is also due to the nature of refractions and reflections within the material itself. This behavior agree with the results of researchers[87].

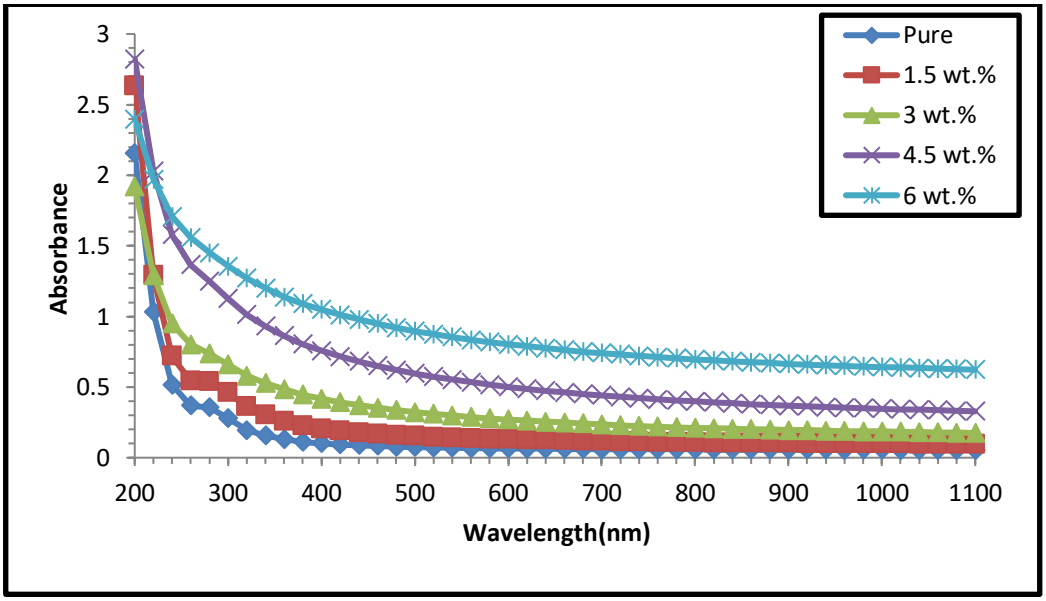

Fig.(4.3). Optical absorbance performance for PVA and PVA/Y_2O_3 nanostructures films with photon wavelength.

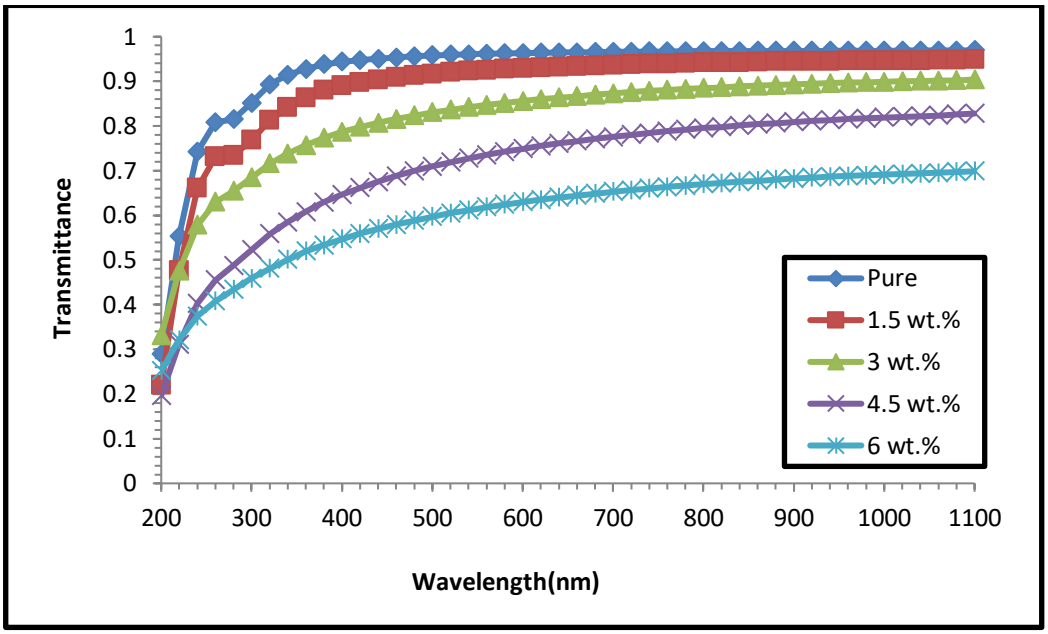

Fig.(4.4). Behavior of optical transmittance for PVA and PVA/Y_2O_3 nanostructures films with photon wavelength.

4.3.2 The Absorption Coefficient of (PVA-Y_2O_3) Nanocomposites

The absorption coefficient of nanocomposites is calculated by using equation (2-5). Figure (4.5) shows the variation of absorption coefficient for (PVA/Y_2O_3) nanocomposites as a function of photon energy of the incident light. As shown in the figure, the absorption coefficient of the samples for (PVA/Y_2O_3) nanocomposites are high at high photon energies. This means that the electron transition has high possibility; i.e., the energy of incident photon is enough to transit the electron from the valence band to the conduction band, which due to the energy of the incident photon is greater than the energy band gap. The absorption coefficient assists to know the nature of electron transition[83,84]. When the values of the absorption coefficient of material are high ($\alpha>10^4$ cm^{-1}), it is expected that direct transition of electron. While, when the values of the absorption coefficient of material are low ($\alpha<10^4$ cm^{-1}), it is expected that

indirect transition of electron. The values of absorption coefficient of (PVA/Y_2O_3) nanocomposites are low ($\alpha<10^4$ cm^{-1}); the transition of electron is indirect. The absorption coefficient of nanocomposites increased with the increasing of the concentrations of nanoparticles. this result agrees with researchers [88].

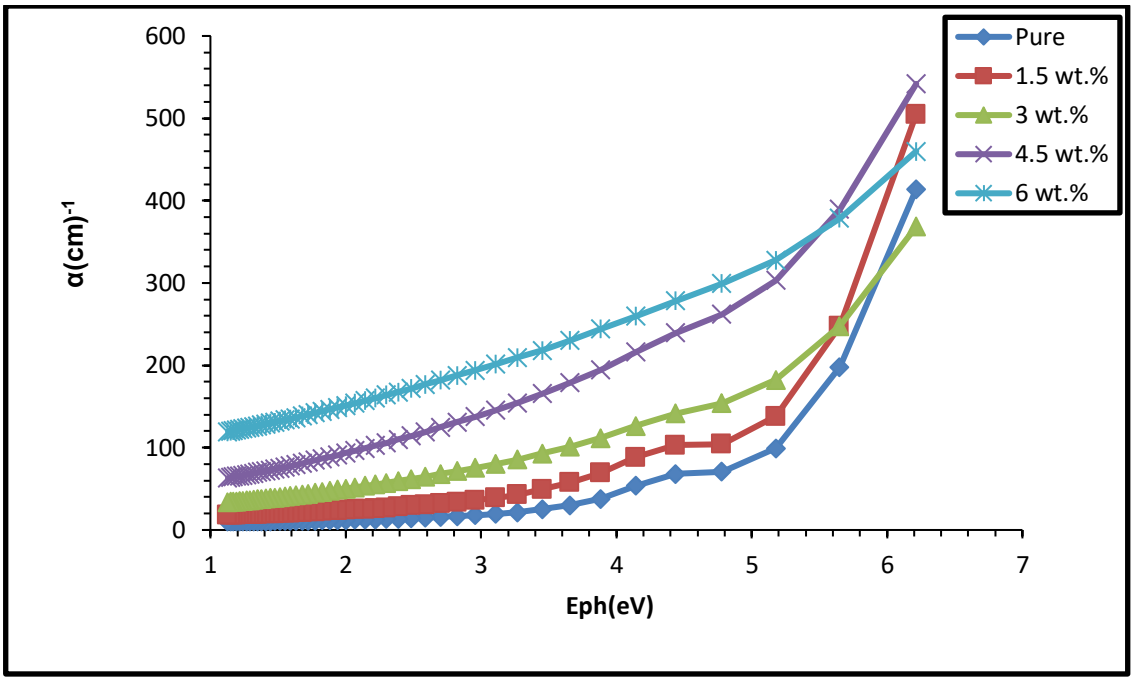

Fig. (4.5). Absorption coefficient behavior for PVA and PVA-Y_2O_3nanostructures with photon energy.

4.3.3 Optical energy gap

The energy band gap of (PVA/Y_2O_3) nanocomposites was calculated by using equation (2.19). The energies gaps for allowed indirect transitions of (PVA/Y_2O_3) nanocomposites are shown in figure (4.6). The energies gaps for forbidden indirect transitions of (PVA/Y_2O_3) nanocomposites are shown in figure (4.7). The energies gaps for allowed and forbidden indirect transitions of (PVA/Y_2O_3) nanocomposites were decreased with increasing the (Y_2O_3) nanoparticles concentrations, this behavior is due to the creation of levels in the energy gap; the transition of electron in this case is conducted in two stages that

involve the transition from the valence band to the generated levels in the energy gap and to the conduction band [89,90], as a result of increasing the (Y_2O_3) nanoparticles concentrations. The electronic conduction depends on (Y_2O_3) nanoparticles concentrations. These results are in agreement with the results of the researcher[90]. The increase in the concentrations of (Y_2O_3) nanoparticles gives electronic paths in the polymer, so the electron moves from the valence band to the conduction band, which explains the decreasing in the energy gap with the increase in the concentration of (Y_2O_3) nanoparticles. These results agreement with researchers finding [90, 91]. The values of the energies gaps for allowed and forbidden indirect transformations are shown in the Table (4-1).

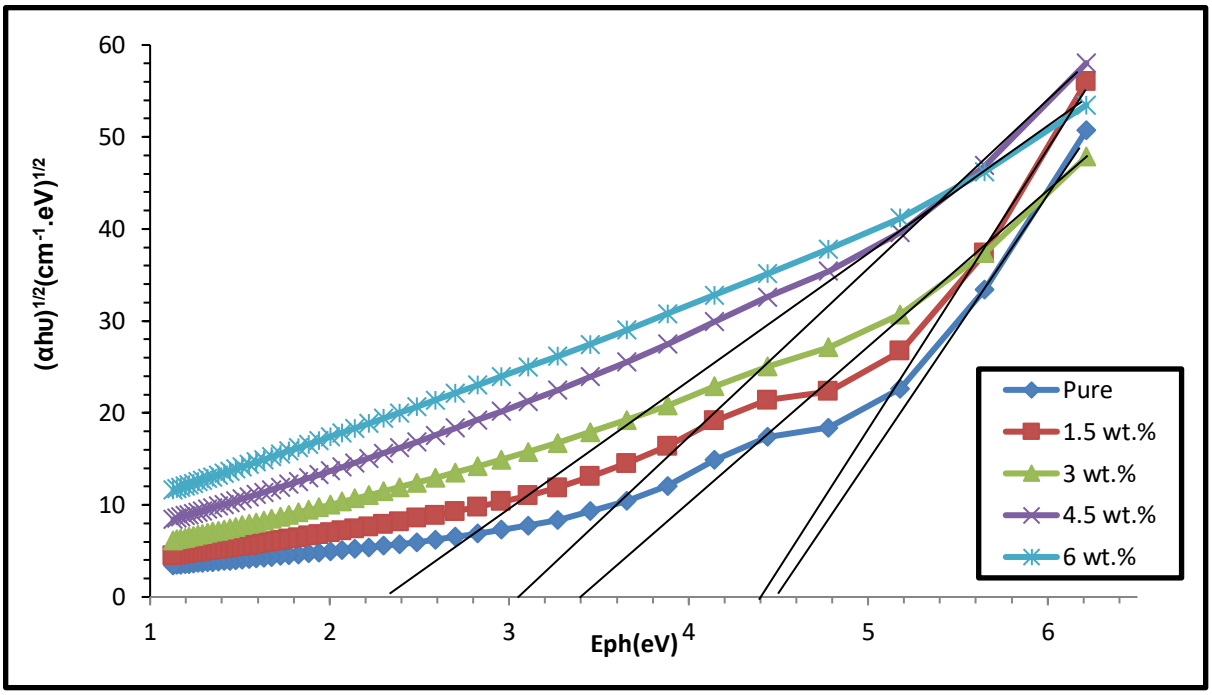

Fig(4.6).Energy gap values of allowed indirect transition for pure PVA and PVA/Y_2O_3 nanostructures.

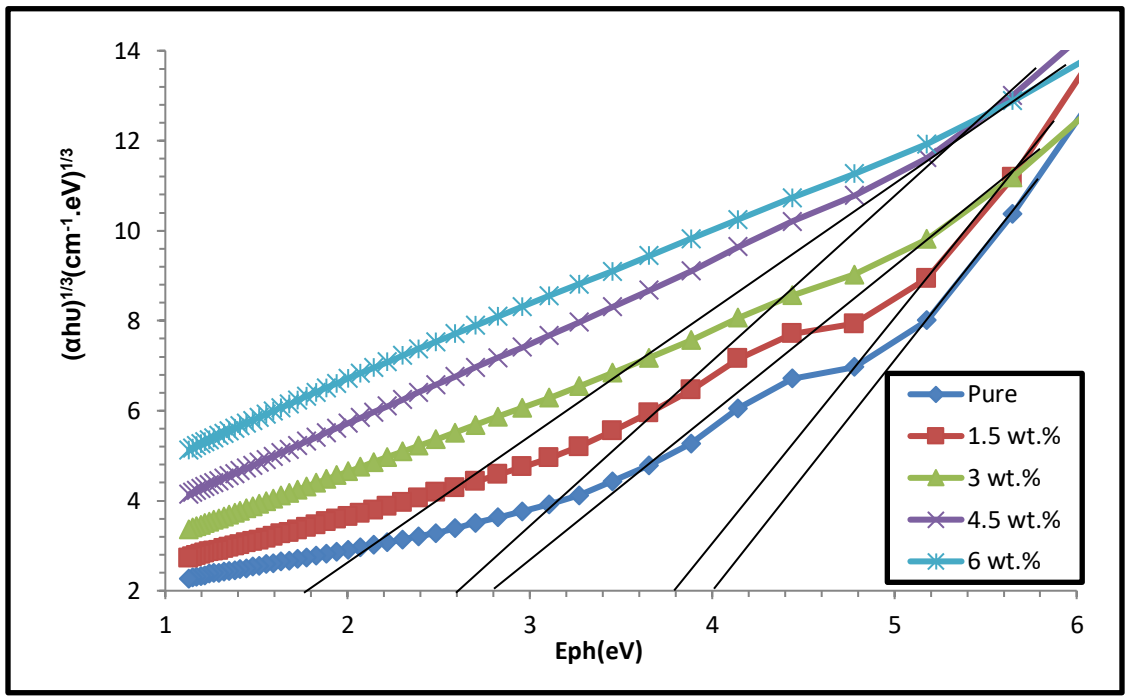

Fig. (4.7): Energy gap values of forbidden indirect transition of PVA/Y_2O_3 nanostructures.

Table (4-1) the values of the energies gaps for allowed and forbidden indirect transformations of (PVA/Y_2O_3) nanocomposites.

Concentration percentage wt.% of Y_2O_3	Allowed energy gap (eV)	forbidden energy gap (eV)
0	4.5	4
1.5	4.4	3.8
3	3.4	2,8
4.5	3.08	2.6
6	2.38	1.8

4.3.4 Extinction coefficient(k)

The extinction coefficient (k) for PVA and (PVA/Y_2O_3) nanocomposite was calculated using equation (2-9). Figure (4.8) shows the change of the extinction coefficient (PVA/Y_2O_3) as a function of wavelength. The figure showed that extinction coefficient increased with increasing the concentration of (Y_2O_3) nanoparticles, this is due to the increasing in optical absorption and photons dispersion in the polymer matrix. Through equation (2-9) that the extinction coefficient depends on the absorption coefficient, and that the extinction coefficient has high values in the UV- region and it increases with increasing wavelength in the visible spectrum region and continues to the near infrared spectrum region. This is due to an increased in the absorption coefficient with increasing of (Y_2O_3) nanoparticles concentration. These results are in agreement with the results of the researcher [92].

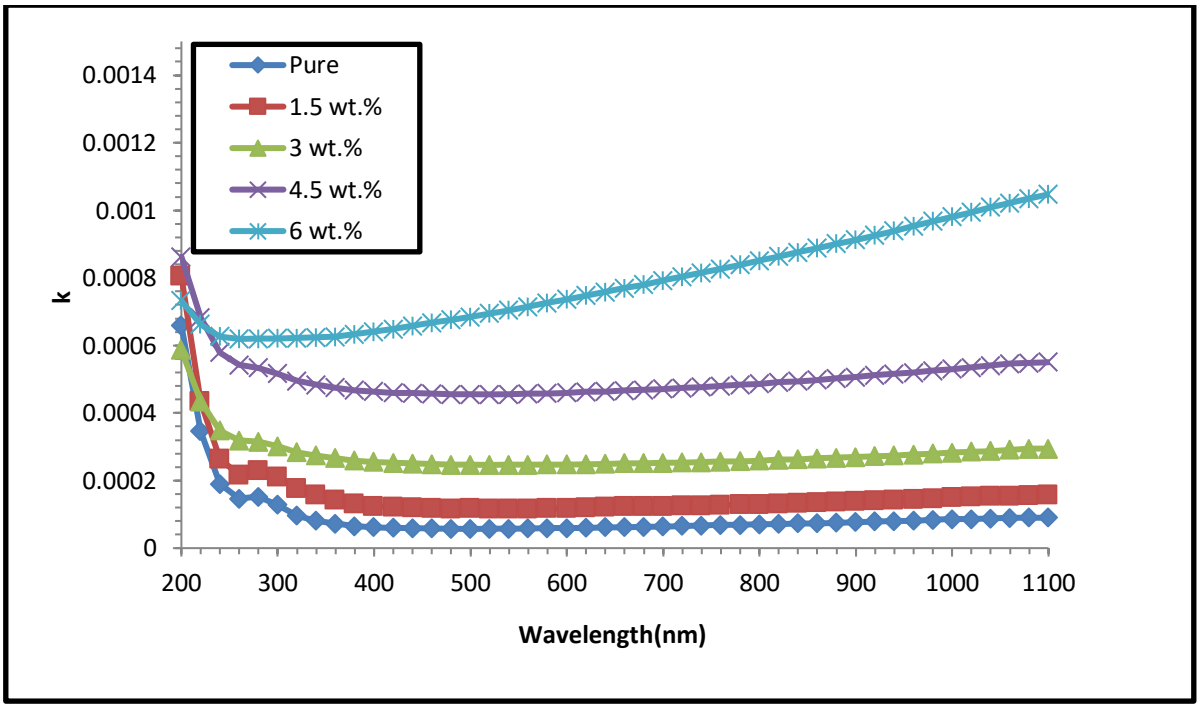

Fig(4.8). Extinction coefficient variation for PVA and PVA/Y_2O_3 nanostructures with photon wavelength.

4.3.5 Refractive Index (n)

The refractive index of (PVA/Y_2O_3) nanocomposite was calculated by using equation (2-8). Figure (4.9) shows the change of the refractive index of (PVA/Y_2O_3) nanocomposite versus as a function of wavelength. As shown in figure, the refractive index of (PVA/Y_2O_3) nanocomposites increased with increasing concentrations of (Y_2O_3) nanoparticles, also it is decreased with the increaseing of the wavelength, due to the increase in the density of nanocomposites [93]. When the incident light interacts with a sample has high refractivity at UV region, the values of refractive index will be increased. These results are in agreement with the results of the researcher[94].

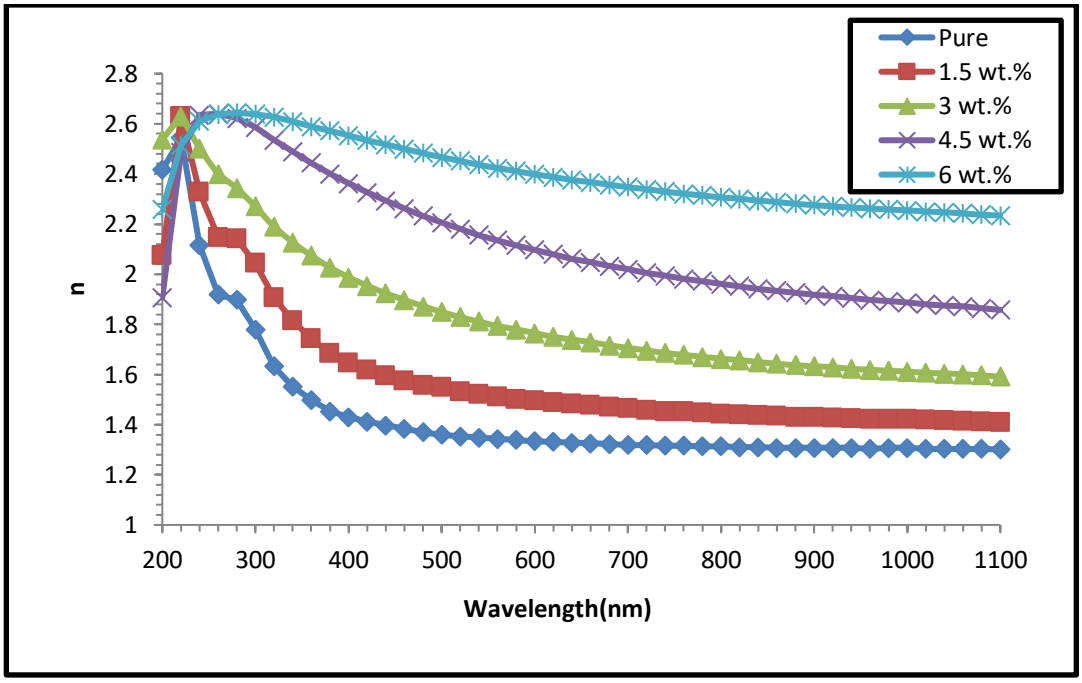

Fig.(4.9) Refractive index variation for PVA and PVA/Y_2O_3 nanostructures with photon wavelength.

4.3.6 Real and Imaginary Parts of Dielectric Constant for PVA and PVA/Y_2O_3 Nanocomposites

The real and imaginary parts of the dielectric constant are calculated using equations (2-13) and (2-14), respectively. Figures (4.10) and (4.11) show change of the real and imaginary parts of dielectric constant with the wavelength of the (PVA/Y_2O_3) nanocomposites. Figure (4.10) shows change of the real parts of the dielectric constant of (PVA/Y_2O_3) with wavelength. The real part of the dielectric constant depends on the refractive index because the extinction coefficient was very small. That are, real dielectric constant was increased with increasing of the (Y_2O_3) nanoparticles concentrations[85]. The effect of (Y_2O_3) nanoparticles on the imaginary part of dielectric constant was shown in Figure (4.11) .The figure shows that imaginary part of dielectric constant of (PVA/Y_2O_3) nanocomposites were increased with increasing of (Y_2O_3) nanoparticles concentrations, this behavior attributed to the increase of electrical polarization, due to contribution of nanoparticles concentration in the sample and increase in charges within the polymers [92].The imaginary part of dielectric constant depends on extinction coefficient especially in the visible and near infrared regions of wavelength, where the refractive index is approximately constant while extinction coefficient increased with the increase of the wavelength[93].

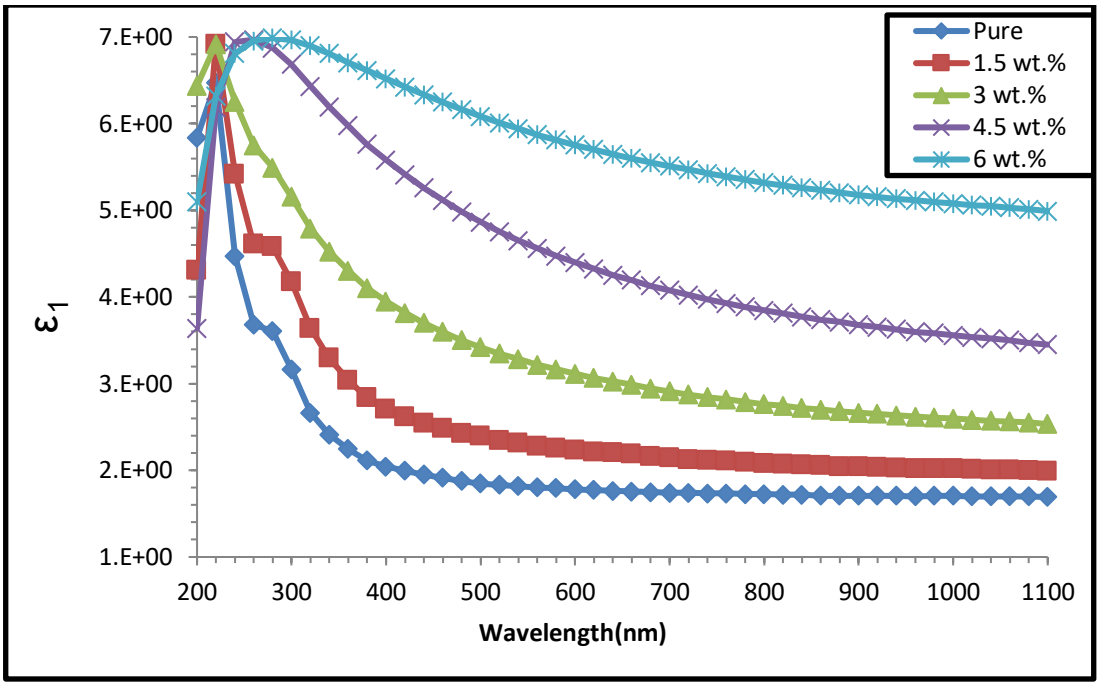

Fig. (4.10) The real part of dielectric constant for PVA and PVA/Y_2O_3 nanostructures with photon wavelength.

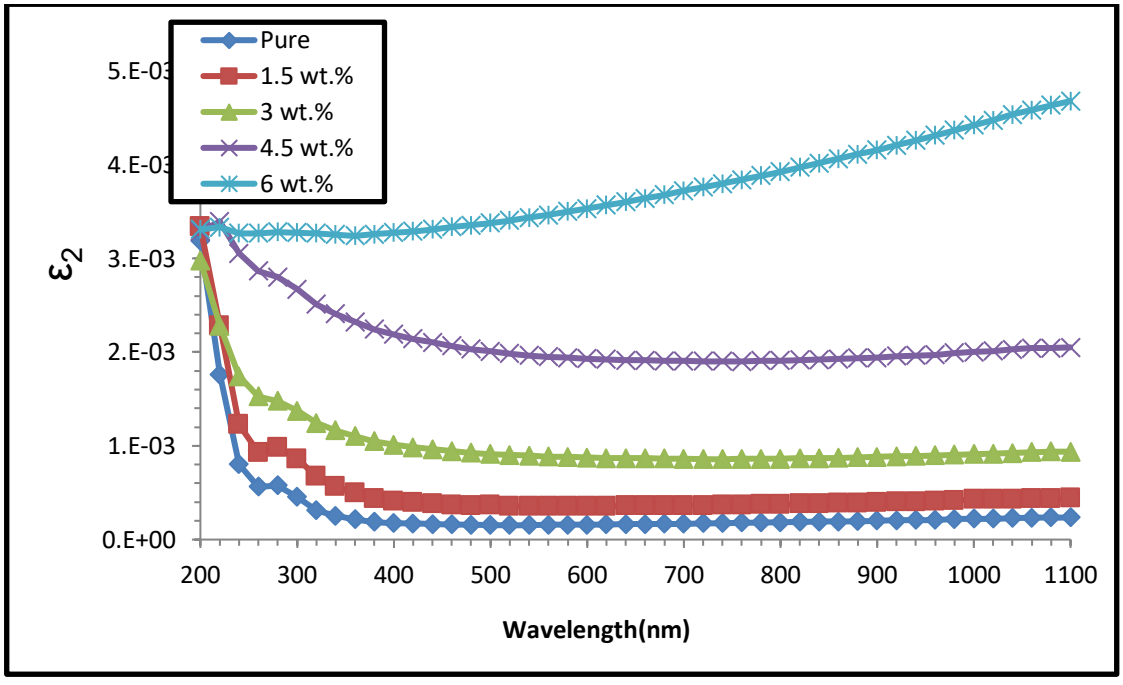

Fig. (4.11) The imaginary part of dielectric constant for PVA and PVA/Y_2O_3 nanostructures with photon wavelength.

4.3.8 Optical Conductivity (σ_{op})

The optical conductivity was calculated using equation (2.15). Figure (4.12) shows the relationship between optical conductivity and wavelength of (PVA/Y_2O_3) nanocomposites. It was observed that the optical conductivity increased as the percentages of (Y_2O_3) in the (PVA) increased to (6 wt.%). This increasing due to the creation of new levels in the band gap leads to facilitate the crossing of electrons from the valence band to these local levels to the conduction band, consequently the band gap decreased, and the conductivity increased [94].

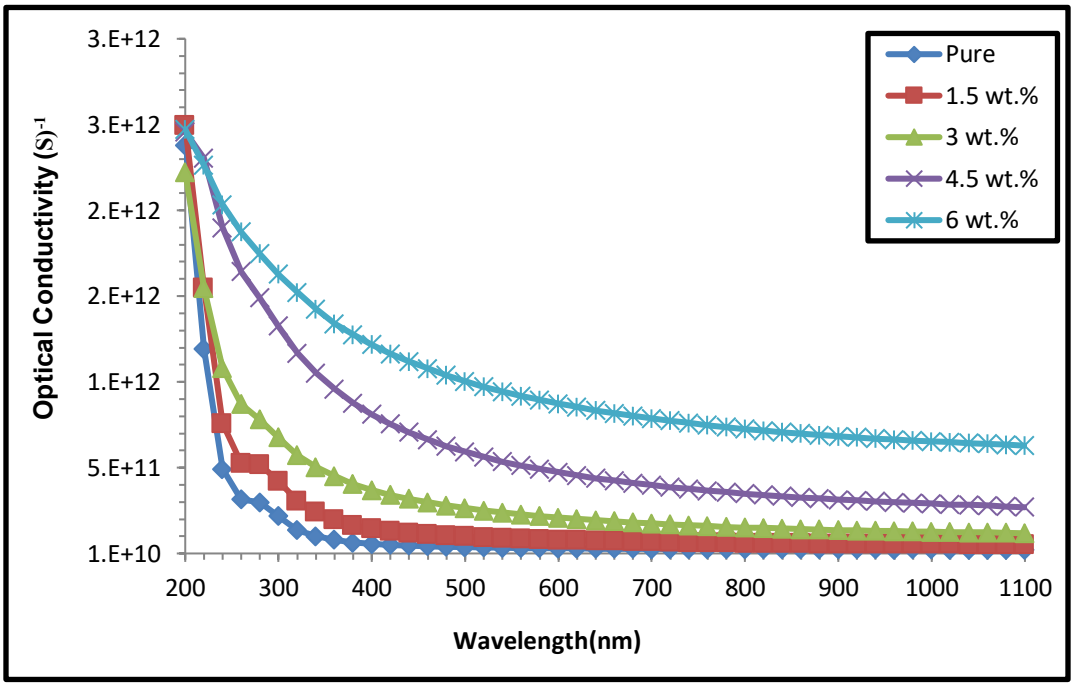

Figure (4.12) Relationship between optical conductivity and wavelength of (PVA/Y_2O_3) nanocomposites.

4.4 - The Electrical Properties of Samples

Alternative current (A.C.) electrical properties for the (PVA/Y_2O_3) nanocomposites were studied within frequency ranging from (100Hz-5MHz) at room temperature. The dielectric constant, which is the most important of A.C properties were calculated using equation (2.34). The dielectric loss was calculated by equation (2.33), using the measured dielectric constant and (tan δ), while the A.C electrical conductivity σ A.C was calculated by equation (2.36) after substituting the measured values of (έ).

4.4.1 - The Dielectric Constant for (PVA/Y_2O_3) Nanocomposites

The variation of dielectric constant for (PVA/Y_2O_3) nanocomposite with frequency for all specimen are shown in Figure (4.13). Due to the various polarization states, it is evident from the data that the dielectric constant will decreased as the frequency applied rises. However, at low frequencies, the polarization of the space charge significantly contributes to increasing the dielectric constant. As the frequency of the electrical field increases, polarization contributes less to the increase in frequency and does so more. This action causes a decrease in the values of the dielectric constant for all samples, and the other forms of polarizations occur at higher frequencies as a result. This was caused by the fact that an ion has a mass higher than an electron. Electronic polarization is the only type of polarization that can occur at higher frequencies because of this difference in mass, which allows electrons to respond to field vibrations even at the highest frequencies [95].

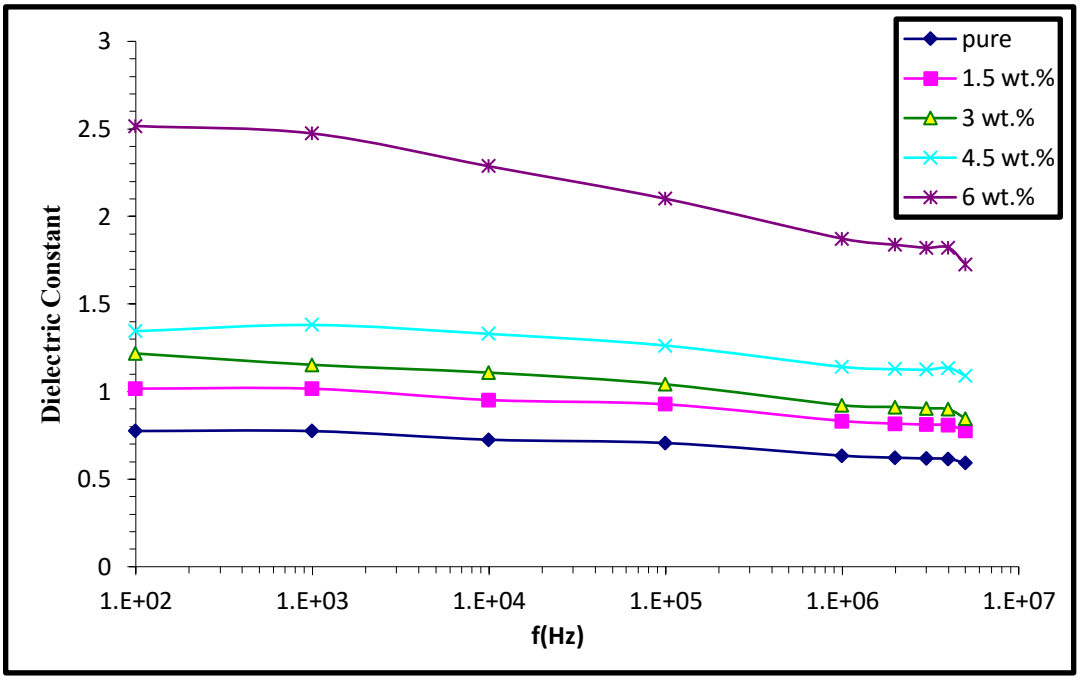

Figure (4.13): Variation of the dielectric constant of (PVA/Y_2O_3) nanocomposites with frequency (Hz).

Figure (4.14) illustrates the effect that adding yttrium oxide nanoparticle (Y_2O_3 NPs) on the dielectric constant at frequency 100 Hz. It is plain to see that the dielectric constant increased in direct proportion to an increasing in Y_2O_3 NPs concentration. This might be because inside the nanocomposite, Y_2O_3 NPs form a continuous network. The microscopically captured images of these nanocomposites made this very evident. This is agree with researchers finding [96,97].

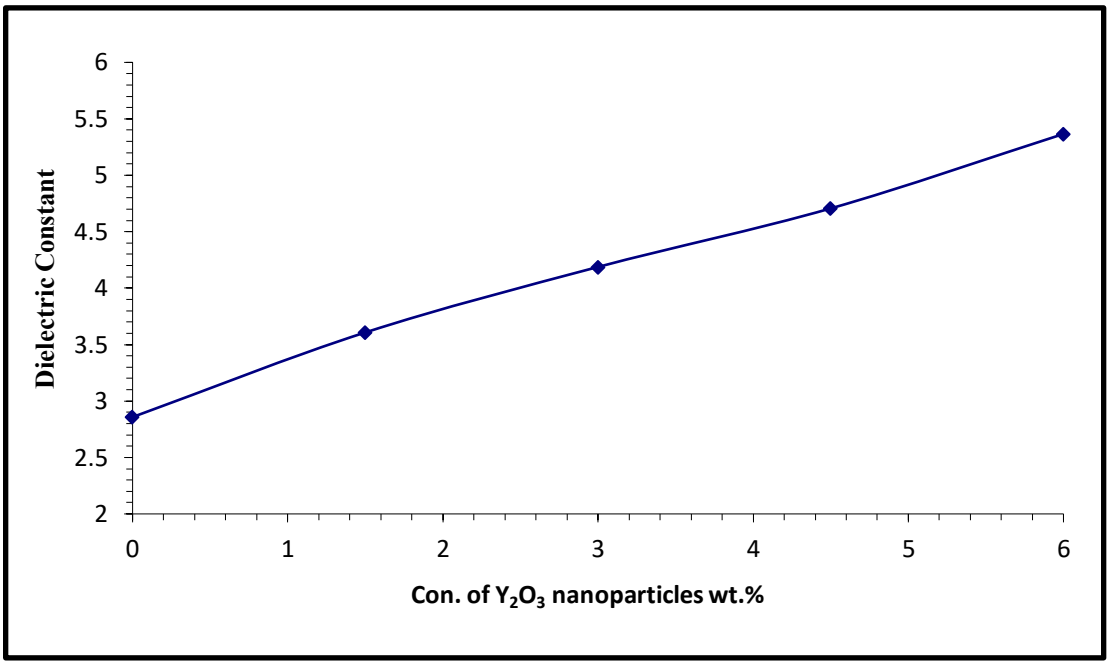

Figure(4.14): Variation of dielectric constant with concentration of Y_2O_3 at 100Hz of (PVA/Y_2O_3) nanocomposites.

4.4.2 The Dielectric Loss of (PVA/Y_2O_3) Nanocomposites

The dielectric loss for PVA and (PVA/Y_2O_3) nanocomposite as a function of frequency are shown in figure (4.15). This figure demonstrates that the dielectric loss of nanocomposites (PVA/Y_2O_3) decreased with an increasing in the frequency of applied electric field. When the frequency increases, there is a relatively modest change in the amount of dielectric loss. This is because various types of polarization are able to take place at high frequencies [98]. As demonstrated in Figure (4.16), increasing in the concentration of Y_2O_3 led to increase in the number of ionic charge carriers, which in turn led to increase in the value of dielectric loss. This phenomenon can be observed when the weight percent content of nanoparticles is increased, this is agreed with the results [99].

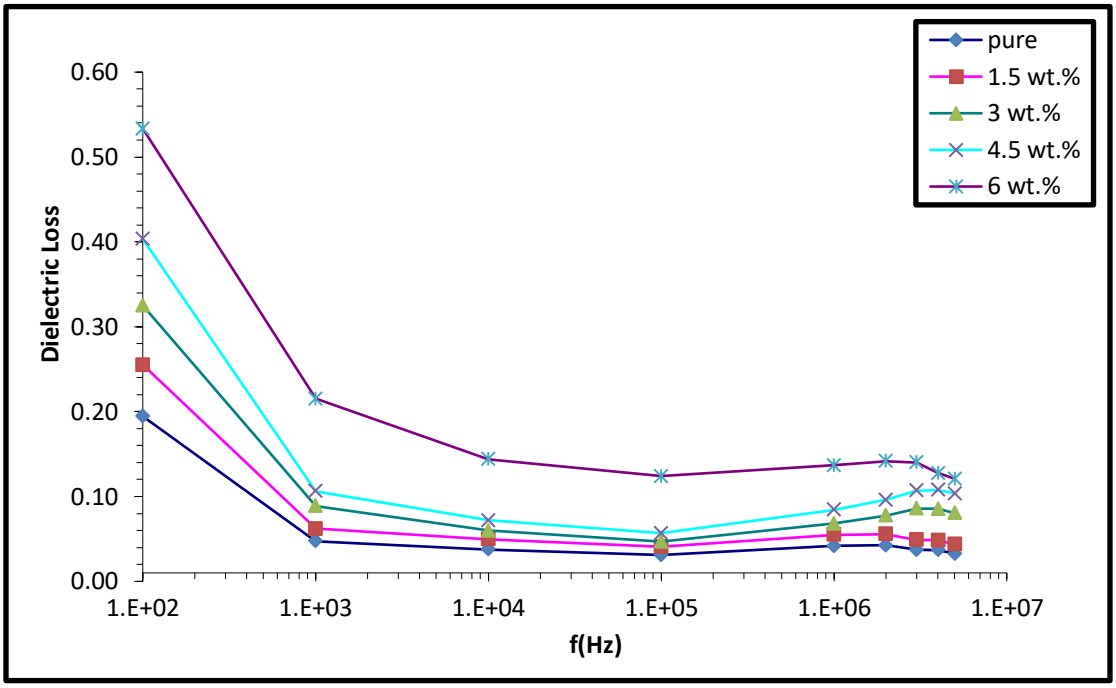

Figure (4.15): Variation of the dielectric loss for PVA and (PVA/Y_2O_3) nanocomposites with frequency(Hz).

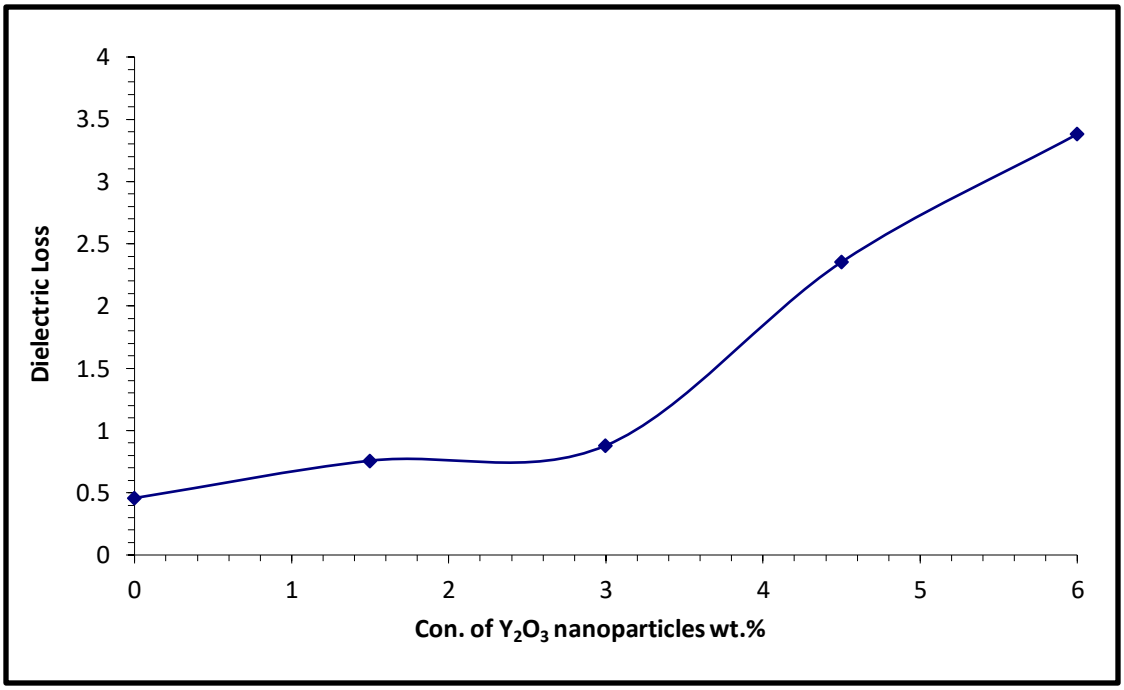

Figure (4.16): Variation of dielectric loss with concentration of Y_2O_3 at 100Hz of (PVA/Y_2O_3) nanocomposites.

4.4.3 The A.C Electrical Conductivity of (PVA/Y_2O_3) nanocomposites.

The variation of A.C electrical conductivity as a function of frequency for (PVA/Y_2O_3) are shown in Figure (4.17). This Figure demonstrates that the electrical conductivity of nanocomposites increased with increasing the frequency, this is due to the hop-up of charge carriers in the localized state and also to the excitation of charge carriers in the conduction band in the upper regions. Two influences that affect A.C conductivity are main chain motion and ion motion, in other words, the increasing in A.C electrical conductivity at low frequency area can be related to interfacial polarization while the increase in conductivity was due to the passage of electrons at frequencies, intermediate and the high. This result agree with other researchers [95].

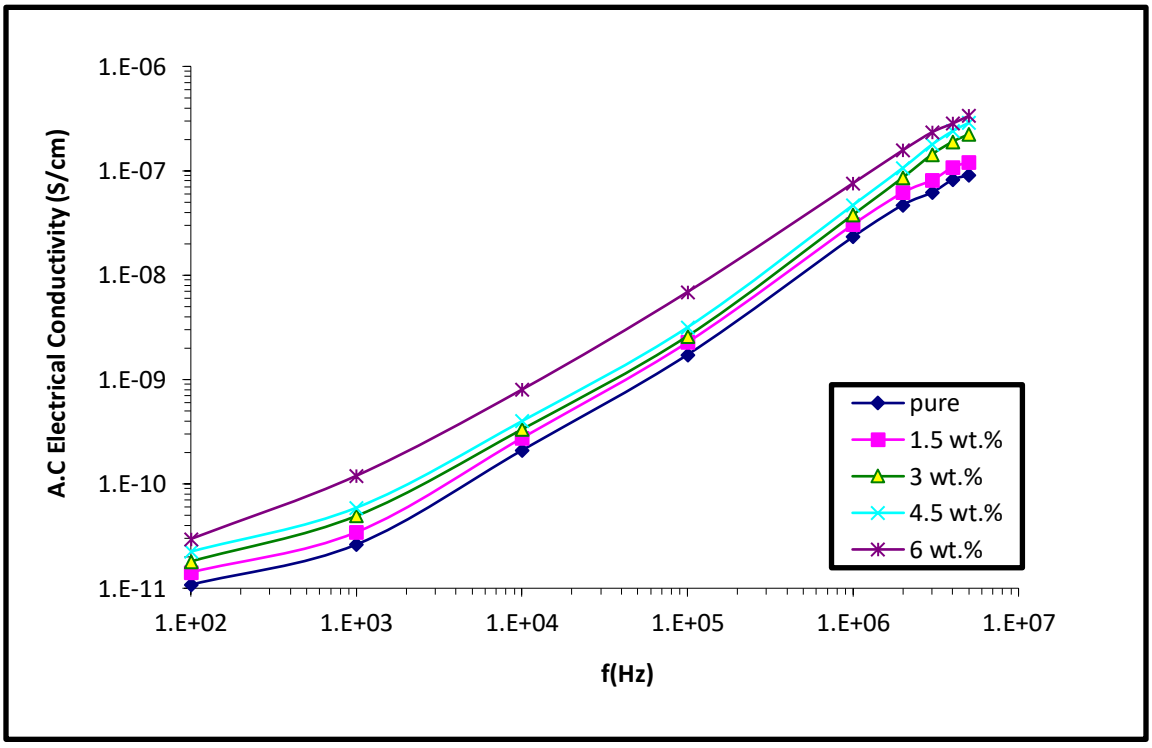

Figure (4.17): Variation of the A.C electrical conductivity with frequency (Hz) for(PVA/Y_2O_3) nanocomposites.

Figures (4.18) show the variation between AC electrical conductivity with concentration of Y_2O_3 nanoparticles. from this figure, it can obtain that the AC electrical conductivity increased with increasing concentration of Y_2O_3 nanoparticles. This occurs as a result of an increase in the number of ionic charge carriers as well as the formation of a continuous network of Y_2O_3 NPs within the composites, these results agree with other researchers [99].

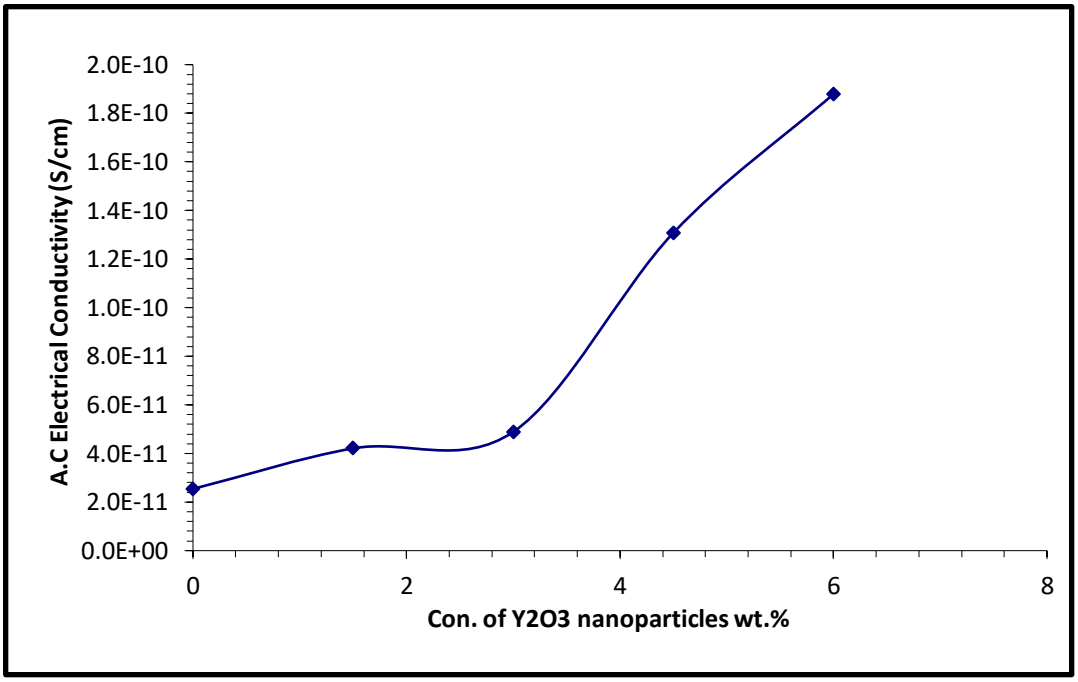

Figure (4.18): Variation of AC electrical conductivity with concentration of Y_2O_3 at 100Hz of (PVA/Y_2O_3) nanocomposites.

4.5 Conclusions

From the obtained results and discussions, the following points are concluded:

1- The optical microscope images showed that the pure PVA was homogenous and with increasing concentration at 6 wt.%, lead to formation path inside the polymer matrix.

2- The FTIR spectra show peaks for the pure PVA and with added Y_2O_3 NPs, to the polymer PVA, there is no peaks exhibited, which means the physical interaction was happened.

3- The absorbance of (PVA/Y_2O_3) nanocomposite increased as the concentrations of (Y_2O_3) nanoparticles increased, while the transmittance and energy gap of (PVA/Y_2O_3) nanocomposite decreased with increasing concentrations of (Y_2O_3) nanoparticles. The absorption coefficient, extinction coefficient, refractive index, real and imaginary parts of dielectric constants and optical conductivity are increasing with the increase of the weight percentages of Y_2O_3 nanoparticles. this give as good indicator these samples could be used as filters of camera lenses or in drugs containers.

4- The dielectric constant, dielectric loss, and A.C electrical conductivity of (PVA/ Y_2O_3) nanocomposite increased with increasing concentrations of (Y_2O_3) nanoparticles, while dielectric constant and dielectric loss decreased as frequency increased, also A.C electrical conductivity increased with an increasing in the frequency. The advantage of enhancement in electrical properties of (PVA/Y_2O_3) nanocomposite that might be used in electronics device.

4.6 Future Works

1- Studying the effect of radiation on some physical properties of (PVA/Y_2O_3) nanocomposites.

2- Studying the thermal and mechanical properties of (PVA/Y_2O_3) nanocomposites.

3- Studying the rheological properties of (PVA/Y_2O_3) nanocomposites.

4- Application of (PVA/Y_2O_3) for Antibacterial.

References

[1] A. P. Mouritz and A. G. Gibson, “Fire Properties of Polymer Composite Materials”, Solid Mechanics and Its Applications, Vol. 143, pp.1-18, (2007).

[2] P. U. Asogwa, “Effect of deposition medium on the optical and solid state properties of annealed MnO2 thin films”, J. of optoelectronics and biomedical materials, Vol. 2, pp.109-117, (2010).

[3] J. E. Mark, “Physical properties of polymers handbook”, Springe, Vol. 107, p.825, (2007).

[4] S. Logothetidis, “Nanostructured Materials and Their Applications”, NanoScience and Technology, pp.1-23, (2012).

[5] M. Köhler and W. Fritzsche, “Nanotechnology an Introduction to Nano structuring Techniques”, 2nd Ed, Completely Revised, (2008).

[6] A. T. Bell, “The Impact of Nanoscience on Heterogeneous Catalysis”, Sci., Vol. 299, No. 5613, pp.1688-1691, (2003).

[7] K. A. Shenoy, “Effects Of Multi-Wall Carbon Nanotubes On The Mechanical Properties Of Polymeric Nanocomposites”, M.Sc. Thesis, Department of Mechanical Engineering and the Faculty of the Graduate School of Wichita State University, (2008).

[8] S. Mustafa, “Engineering Chemistry”, Library of Arab society for pub. and dis, Jordan, (2008).

[9] A. C. Long and M. J. Clifford, “Composite forming mechanisms and materials characterization”, Composites forming technologies, pp.1-21, (2007).

[10] A. Mohaisen, “Study of electrical conductivity for amorphous and semi crystalline polymers filled with Lithium Fluoride Additive”, M. Sc. Thesis, University of Mustansiriah, College of Science, (2009).

[11] J. M. Schultz, “Polymer materials science”, Prentice Hall, (1974).

[12] S. Amin and M. Amin, “Thermoplastic Elastomeric (Tpe) Materials and Their Use in Outdoor Electrical Insulation”, Rev. Adv. Mater. Sci.,Vol. 29, pp.15-30, (2011).

[13] A. H. Doulabi, K. Mequanint, and H. Mohammadi, “Blends and nanocomposite biomaterials for articular cartilage tissue engineering,” Materials (Basel)., Vol. 7, No. 7, pp. 5327–5355, (2014).

[14] P. M. Ajayan, P. Redlich, and M. Ru¨ hle, “Structure of carbon nanotube-based nanocomposites,” J. Microsc., Vol. 185, No. 2, pp. 275–282, (1997).

[15] J. Robertson, “Realistic applications of CNTs,” Mater. Today, Vol. 7, No. 10, pp. 46–52, (2004).

[16] E. Tang, G. Cheng, and X. Ma, “Preparation of nano-ZnO/PMMA composite particles via grafting of the copolymer onto the surface of zinc oxide nanoparticles,” Powder Technol., Vol. 161, No. 3, pp. 209–214, (2006).

[17] H. Gao, B. Ji, I. L. Jäger, E. Arzt, and P. Fratzl, “Materials become insensitive to flaws at nanoscale: lessons from nature,” Proc. Natl. Acad. Sci., Vol. 100, No. 10, pp. 5597–5600, (2003).

[18] W. D. Callister, “An introduction: material science and engineering,” John Wiley Sons Inc, Vol. 23, No. 12, pp. 2408–2418, (2007).

[19] J. Paull, “Nanotechnology, No Free Lunch,” Vol. 62, No. 15, pp. 3418–3424, (2010).

[20] C. Demerlis and D. Schoneker, “Review of the oral toxicity of polyvinyl alcohol (PVA)”, Food Chem. Toxicol, Vol. 41, No. 3, pp. 319–326, (2003).

[21] C. Ravindra, M. Sarswati, G. Sukanya, P. Shivalila, Y. Soumya, and K. Deepak, “Tensile and thermal properties of poly (vinyl) pyrrolidone/vanillin incorporated polyvinyl alcohol films”, Res. J. Phys. Sci., Vol. 3, No. 8, pp. 1–6, (2015).

[22] k. Choo, Y. C. Ching, C. H. Chuah, S. Julai, and N. S. Liou, “Preparation and characterization of polyvinyl alcohol-chitosan composite films reinforced with cellulose nanofiber”, Materials, Vol. 9, No. 8, p.644. (2016).

[23] I. Sakurada, “Polyvinyl Alcohol Fibers”, Taylor & Francis, of International Fiber Science and Technology, Vol. 6, p. 472, (1985).

[24] S. S. Chiad, S. F. Oboudi, K. H. Abass, and N. F. Habubi,“Characterization of Silver/Polyvinyl Alcohol (Ag/PVA) Films prepared by Casting Technique”, Iraqi J. of Polymers, Vol. 16, No. 2, pp.10-18, (2012).

[25] A. Gautam and S. Ram, “Preparation and thermomechanical properties of Ag-PVA nanocomposite films”, Mater. Chem. Phys., vol. 119, No. 2, pp. 266–271, (2010).

[26] Z. H. Mbhele, M. G. Salemane, C. G. E. Van Sittert, J. M. Nedeljković, V. Djoković and A. S. Luyt, A. S., "Fabrication and characterization of silver− polyvinyl alcohol nanocomposites" Chemistry of Materials, Vol. 15, No. 26, pp.5019-5024, (2003)

[27] H. Ahmed and A. Hashim, "Geometry optimization, optical and electronic characteristics of novel PVA/PEO/SiC structure for electronics applications" Silicon, Vol. 13, No.8, pp. 2639-2644, (2021).

[28] A. M. Kadim, K. H. Abass and A. J. Alrubaie, "Structure and optical properties of Ag content polymeric blend" AIP Conference Proceedings, Vol. 2398, No. 1, p.020036, (2022).

[29] B. Mohammed, H. Ahmed, A. Hashim, A. ,"Studies on Polymer Blend/BaTiO3 Nanocomposites for Industrial and Biological Applications" Journal of Applied Sciences Research, Vol.18, No. 2, pp.1-10, (2022).

[30] G. Mohammed, A. M. El Sayed, and W. M. Morsi, "Spectroscopic, thermal, and electrical properties of MgO/polyvinyl pyrrolidone/polyvinyl alcohol nanocomposites"Journal of Physics and Chemistry of Solids, Vol. 115, pp.238-247, (2018).

[31] M. Liu, B. Guo, M. Du, and D. Jia, “Drying induced aggregation of halloysite nanotubes in polyvinyl alcohol/halloysite nanotubes solution and its effect on properties of composite film,” Appl. Phys. A, vol. 88, no. 2, pp. 391–395, 2007.

[32] X. J. Wang, L. D. Zhang, J. P. Zhang, G. He, M. Liu and L. Q. Zhu, "Effects of post-deposition annealing on the structure and optical properties of Y_2O_3 thin films" Materials Letters, Vol.62, No. 26, pp. 4235-4237, (2008).

[33] Z. A. Al-Ramadhan, J. Abdulsattar , H. Abdul and K. Hmud," Optical and Morphological Properties of (PVA-PVP-Ag) Nanocomposites, International Journal of Science and Research (IJSR),Vol. 5,No.3 pp. 1828-1836, (2016).

[34] H. T. Salloom, A. S. Jasim and T. K. Hamad, "synthesis and optical characterization of Ag/PVA nanocomposites films" Al-Nahrain Journal of Science, Vol.20, No.4, pp. 56-63, (2017).

[35] W. W. Zhang, W. P. Zhang, P. B. Xie, M. Yin, H. T. Chen, L. Jing, S. D. Xia, S. D.,"Optical properties of nanocrystalline Y_2O_3: Eu depending on its odd structure" Journal of colloid and interface science, Vol. 262, No.2, pp. 588-593, (2003).

[36] G. Rajakumar, L. Mao, T. Bao, W. Wen, S. Wang, T. Gomathi and X. Zhang, "Yttrium oxide nanoparticle synthesis: an overview of methods of preparation and biomedical applications" Applied Sciences, Vol.11, No.5, p.2172, (2021).

[37] S. Balakrishnan, K. Ananthasivan, K. C. H. Kumar, "Studies on the synthesis of nanocrystalline yttria powder by oxalate deagglomeration and its sintering behavior" Ceram. Int., Vol.41, pp.5270–5280, (2015).

[38] Q. Jebur, A. Hashim and M. Habeeb, "Structural, AC electrical and optical properties of (polyvinyl alcohol–polyethylene oxide–aluminum oxide) nanocomposites for piezoelectric devices" Egyptian Journal of chemistry, Vol. 62, pp.719-734, (2019).

[39] S. N. Bagayev, V. V. Osipov, V. A. Shitov, E. V. Pestryakov, V. S. Kijko, R. N. Maksimov and V. V. Petrov, V. V. ,"Fabrication and optical properties of Y2O3-based ceramics with broad emission bandwidth", Journal of the European Ceramic Society, Vol. 32, No.16, pp.4257-4262, (2012).

[40] S. Som, S. K. Sharma and S. P. Lochab, "Swift heavy ion induced structural and optical properties of Y_2O_3: Eu^{3+} nanophosphor" Materials Research Bulletin, Vol.48, No.2, pp. 844-851, (2013).

[41] H. S. Rasheed," The effect of Adding (ZrC) Nanoparticles to (PVP-PVA) Blend on their Optical properties for Humidity Sensor Application," Journal of Physics: Conference Series, Vol.1660, (2020).

[42] S. Sugumaran, C. S. Bellan, and M. Nadimuthu, “Characterization of composite PVA–Al_2O_3 thin films prepared by dip coating method,” Iran. Polym. J., Vol. 24, No. 1, pp. 63–74, (2015).

[43] J. J. Mathen, G. P. Joseph, and J. Madhavan, “Improving the optical and dielectric properties of PVA matrix with nano-ZnSe: Synthesis and Characterization,” Int. J. Eng. Res, Vol. 4, pp. 1054–1062, (2016).

[44] M. A. Habeeb, L. A. Hamza, "Structural, Optical and DC Electrical Properties of (PVA-PVP-Y_2O_3) Films and Their Application for Humidity Sensor” Journal of Advanced Physics, Vol. 6, Vol.1, pp. 1-9, (2017).

[45] B. Guruswamy, V. Ravindrachary, C. Shruthi, S. Hegde, R. N. Sagar, and S. D. Praveen, “Optical, electrical and thermal properties of SnO2 nanoparticles doped poly vinyl alcohol-poly vinyl pyrrolidone blend polymer electrolyte,” Indian J. Adv. Chem. Sci., Vol. 6, No.1, pp. 17–20,
[46] A. Hashim, Y. Al-Khafaji, and A. Hadi, “Synthesis and Characterization of Flexible Resistive Humidity Sensors Based on PVA/PEO/CuO Nanocomposites”, Trans. Elect. Electron. Mater., Vol.20, No.6, pp. 530–536, (2019).

[47] Q. Jebur, A. Hashim, and M. Habeeb, “Fabrication, Structural and Optical properties for (Polyvinyl Alcohol–Polyethylene Oxide–Iron Oxide) Nanocomposites,” Egypt. J. Chem., Vol. 63, No. 2, pp. 611–623, (2020).

[48] Z. A. Alrowaili, T. A. Taha, K. S. El-Nasser and H. Donya, H., "Significant enhanced optical parameters of PVA-Y_2O_3 polymer nanocomposite films. Journal of Inorganic and Organometallic" Polymers and Materials, Vol. 31, No.7, pp. 3101-3110, (2021).

[49] A. Nain, S. Dahiya, R. P. Chahal and E. Dhanda, "Ultraviolet (UV) irradiated induced changes in optical properties of PVA/Ag nanocomposite films" Physica Scripta, Vol. 97, No. 4, p. 045817, (2022).

[50] A. D. Gianfrancesco, "in Materials for Ultra-Supercritical and Advanced Ultra-Supercritical Power Plants", Woodhead publishing, (2017).
[51] B. Jörgen "Mechanics of Solid Polymers", William Andrew, (2015).

[52] P. Griffiths, J. D. Hasseth,” Fourier Transform Infrared Spectrometry”, (2nd ed.). Wiley-Blackwell, Vol.18, (2007).
[53] K. G. H.´andez Beltr´ and S. E. A. Guti´errez, "Determination of the elastic constants in the classicalvibrational model of the CO_2 molecule”,

Universidad de El Salvador, Facultad de Ciencias Naturales y Matem´atica, Escuela de F´ısica, Analytic Mechanics (2017).

[54] A. Abdulmitalib," Studying in Electric and Optical Properties of Polymers with Application on Non crystal Films from Poly acrylic acid", M.Sc. Thesis, Collage of Science, University of Basrah, (1981).

[55] G. Cao and J. Brinker, "annual review of nano research", (2008).

[56] G. K. Raheem, S. H. Ahmed, " Study Of Optical Properties Of (PEO-PEG) Blends", Journal University of Kerbala, Vol.14, No.4, (2016).

[57] J. Rebok, "Experimental Methods in Polymer Chemistry", John Wiley and Sons, (1980).

[58] O. Stenzel, The physics of thin film optical spectra. Springer, 2015.

[59] M. A. Omer, "Elementary of Solid State Physics", Adison Wesely, Pub., Co. Lon, (1975).

[60] A. D. A. Buba and J. S. A. Adelabu, "Optical and electrical properties of chemically deposited ZnO thin films", The Pacific Journal.of Science and Technology, Vol.11, pp.429-434, (2010).

[61] J. I. Pankove, "Optical processes on semiconductors Dover publication," Inc. New york, 1971.

[62] D. A. Neamen, "Semiconductor Physics and Devices, University of New Mexico, Richard D. Irwin." Inc, 1992.

[63] R. Tintu, K. Saurav, K. Sulakshna, V. P. N. Nampoori, P. Radhakrishnan, and S. Thomas, “Ge28Se60Sb12 / PVA composite films for photonic applications,” J Non-Oxide Glas., Vol. 2, No. 4, pp. 167-174, 2010.

[64] C. Kittle, "Introduction to Solid State Physics", 8th ed. , John Wiley and Sons Inc. , 2005.

[65] C. Mwolfe, N. Holouyak, G.B.Stillman, "Physical properties of Semiconductor", prentice Hall, New York, 1989.

[66] J. I . Pankove, "Optical Process in Semiconductors", Dover Publishing, Inc., New York, 1971.

[67] Y. N. Al-Jamal, "Solid State Physics", Al-Mosel University, (2nd Ed.), Arabic Version, 2000.

[68] S. Karvinen, "The effect of trace element doping of TiO_2 on the crystal growth and on the anatase to rutile phase transformation of TiO_2", Solid State Sci., Vol.5, pp.811-819, (2002).

[69] A. A. Alnajjar, "ZnO: Al grown by sputtering from two different target sources. A comparison study", Advances in condensed matter phys. Article, Vol.2012, (2012).

[70] C M. Y. Nadeem and W. Ahmed, “Optical properties of ZnS thin films,” Turkish J. Phys., vol. 24, no. 5, pp. 651–659, 2000.

[71] J. Tauc, A. Menth, and D. L. Wood, “Optical and magnetic investigations of the localized states in semiconducting glasses,” Phys. Rev. Lett., vol. 25, no. 11, p. 749, 1970.

[72] T. Seghier and F. Benabed, “Dielectric Proprieties Determination of High Density Polyethylene (HDPE) by Dielectric Spectroscopy,” Int. J. Mater. Mech. Manuf., Vol. 3, No.2, pp.121–124, (2015).

[73] S. Shekhar, V. Prasad and S. Subramanyam, "Structural and electrical properties of composites of polymer-iron carbide nanoparticles embedded in carbon,” Mater. Sci. Eng. B Solid-State Mater. Adv. Technol., Vol. 133, No. 1–3, pp. 108–112, (2006).

[74] T. Furukawa, “Electrical properties of polymers,” Reports Prog. Polym. Phys. Japan, Vol. 43, pp. 369–390, (2000).

[75] R. Dorf, The Electrical Engineering Hand Book, CRC Press LLC, 2nd Edition, Piscataway, New Jersey, USA, pp.1-2976 (2000).

[76] L.L.Hench and and J. K. West, Principles of Electronic Ceramics. New York, United States: John Wiley and Sons Ltd, (1990).

[77] R. C. Dorf, The Electrical Engineering Hand Book. New Jersey, USA: CRC Press LLC, (2000).

[78] H. Fröhlich, Theory of dielectrics: dielectric constant and dielectric loss, vol. 190. Oxford University Press, USA, 1958.

[79] A. R. Blythe, T. Blythe, and D. Bloor, Electrical properties of polymers. Cambridge university press, (2005).

[80]A. Jabbar, S. M. Khalil, A. R. Abdulridha, E. Al-Bermany, and K. Abdali, “Dielectric, AC Conductivity and Optical Characterizations of (PVA-PEG) Doped SrO Hybrid Nanocomposites.pdf,” Key Eng. Mater., vol. 936, pp. 83–92, 2022

[81] R. Dorf, The Electrical Engineering Hand Book, CRC Press LLC, 2nd Edition, Piscataway, New Jersey, USA, pp.1-2976 (2000).

[82] N. Rajeswari, S. Selvasekarapandian, S. Karythikeyan, M. Prabu, G. Hirankumar, H. Nithya, C. Sanjeeviraja, "Conductivity and dielectric Properties of (PVA-PVP) poly blend film using non-aqueous medium". Journal of Non- Crystalline Solids, Vol. 357, No. 22, pp. 3751- 3756, (2011).

[83] M. A. Morsi , A. H. Oraby , A. G. Elshahawy, R. M. Abd El- Hady, "Preparation, structural analysis, morphological investigation and electrical properties of gold nanoparticales filled (PVA-CMC) blend",Journal of Materials Research and Technology, Vol.8, No. 6 ,PP. 5996-6010, (2019).

[84] P. Phukan and D. Saikia, "Optical and structural investigation of CdSe quantum dots dispersed in PVA matrix and photovoltaic applications," Int. J. Photoenergy, Vol. 21, No. 10, pp. 43–46, (2013).

[85] G. A. M. Amin and M. H. Abd-El Salam, "Optical, dielectric and electrical properties of PVA doped with Sn nanoparticles," Mater. Res. Express, Vol. 1, No. 2, p.25024, (2014).

[86] A. Abdulmunaim and A. Hashim, "Electronic Transitions For (PS–LiF) Composites," Vol. 21, No. 10, pp. 43–46, (2010).

[87] K. Krishnamoorthy, G. Manivannan, S. J. Kim, K. Jeyasubramanian, and M. Premanathan, "Antibacterial activity of MgO nanoparticles based on lipid peroxidation by oxygen vacancy," J. Nanoparticle Res., Vol. 14, No. 9, pp. 1–10, (2012).

[88] M. Sterrer, T. Berger, O. Diwald, and E. Knözinger, "Energy transfer on the MgO surface, monitored by UV− induced H2 chemisorption," J. Am. Chem. Soc., Vol. 125, No. 1, pp. 195–199, (2003).

[89] N. B. Kumar, V. Crasta, and B. M. Praveen, "Advancement in

microstructural, optical, and mechanical properties of PVA (Mowiol 10-98) doped by ZnO nanoparticles," Phys. Res. Int., Vol. 2014, (2014).

[90] S. Salman, N. Bakr, and M. H. Mahmood, "Preparation and study of some optical properties of (PVA-Ni (CH3COO) 2) composites," Int. J. Curr. Res, Vol. 6, No. 11, pp. 9638–9643, (2014).

[91] A. M. Abdelghany, E. M. Abdelrazek, and D. S. Rashad, "Impact of in situ preparation of CdS filled PVP nano-composite," Spectrochim. Acta Part A Mol. Biomol. Spectrosc., Vol. 130, pp. 302–308, (2014).

[88] D. E. Hegazy, M. Eid, and M. Madani, "Effect of Ni nano particles on thermal, optical and electrical behaviour of irradiated PVA/AAc films," Arab J. Nucl. Sci. Appl., Vol. 47, No. 1, pp. 41–52, (2014).

[89] A. Hashim, M. Husaien, J. H. Ghazi, and H. Hakim, "Characterization of (polyvinyl alcohol–polyacrylamide–pomegranate peel) composite so as biocomposites materials," Univers. J. Phys. Appl., Vol. 1, No. 3, pp. 242–244, (2013).

[90] M. M. El-Desoky, I. M. Morad, M. H. Wasfy, and A. F. Mansour, "Structural and optical properties of TiO2/PVA nanocomposites," IOSR J. Appl. Phys.(IOSR-JAP), Vol. 9, No. 5, pp. 33–43, (2017).

[91] S. F. Bdewi, O. G. Abdullah, B. K. Aziz, and A. A. R. Mutar, "Synthesis, structural and optical characterization of MgO nanocrystalline embedded in PVA matrix," J. Inorg. Organomet. Polym. Mater., Vol. 26,

No. 2, pp. 326–334, (2016).

[92] M. A. Nabi "Effect of nano ZnO on the optical properties of poly (vinyl chloride) films," Int. J. Polym. Sci., Vol. 2014, (2014).

[93] A. Hashim, B. H. Rabee, M. A. Habeeb, N. Abd-alkadhim, and A. Saad, "Study of electrical properties of (PVA-CaO) composites," Am J Sci Res, Vol. 73, pp. 5–8, (2012).

[91] G. Attia and M. F. H. Abd El-kader, "Structural, optical and thermal characterization of PVA/2HEC polyblend films," Int. J. Electrochem. Sci, Vol. 8, No. 4, pp. 5672–5687, (2013).

[92] O. G. Abdullah, "Influence of barium salt on optical behavior of PVA based solid polymer electrolytes," Eur. Sci. J., Vol. 10, No. 33, (2014).

[93] N. K. Abbas, M. A. Habeeb, and A. J. K. Algidsawi, "Preparation of chloro penta amine cobalt (III) chloride and study of its influence on the structural and some optical properties of polyvinyl acetate," Int. J. Polym. Sci., Vol. 2015, 2015.

[94] H. N. Najeeb, " Study of Some Electrical and Optical Properties for Thin Films Prepared from Polymeric Composites ", M.Sc. thesis, College of sciences, University of Babylon, (2011).

[95] K. Rajesh, V. Crasta, N. Rithin Kumar, G. Shetty, and P. Rekha, "Structural, optical, mechanical and dielectric properties of titanium dioxide

doped PVA/PVP nanocomposite," J. Polym. Res., Vol. 26, No. 4, pp1-10, (2019).

[96] M. Harun, E. Saion, and A. Kassim, "Dielectric properties of poly (vinyl alcohol) /polypyrrole composite polymer films," J. Adv. Sci. Arts, Vol. 1, No.2014, pp. 9–16, (2009).

[97] N. Habubi, Z. Al-ramadhan, and R. Khaleel, "(vinyl chloride) modified by nickel ethyl," Proceeding of 3rd scientific conference, No. 24, pp. 2080–2087, (2009).

[98] A. S. Al-Nesrawy and A. Abdulridha, "Synthesis Characterization of (PVA- PVP-C.B) nano composites," Journal of Physics: Conference Series, Vol. 1804, No. 15, pp. 2524–2532, (2020).

[99] Q. Feng, Z. Dang, N. Li, and X. Cao, " Preparation and Dielectric Property of Ag -/PVA Nano-composite", Mater. Sci. Eng. Vol.99, pp.325-328, (2003).

الخلاصة

في هذه الدراسة، حضر المتراكب النانوي PVAالغير مشوب والمشوب بالجسيمات النانوية Y_2O_3 بطريقة الصب بنسب وزنية مختلفة من Y_2O_3 النانوية (0، 1.5، 3 ،4.5 و 6) % .wt . تم تشخيص الخصائص التركيبية والسطحية والبصرية والكهربائية للمتراكب النانوي (PVA/Y_2O_3). تتضمن الخصائص التركيبية المجهر الضوئي والتحليل الطيفي للأشعة تحت الحمراء (FTIR). أظهرت صور المجهر الضوئي توزيع الجسيمات النانوية Y_2O_3بشكل شبكة مستمرة داخل البوليمر عند النسبة (6 wt.%) . اظهر طيف (FTIR) زحف في بعض القمم وزيادة في شدة لقمم اخرى مقارنة مع الغشاء (PVA) وهذا يشير بانه لايوجد تفاعل بين البوليمر والمواد النانوية المضافة. أظهرت نتائج الخصائص البصرية للمتراكب النانوي بأن الامتصاصية، معامل الامتصاص، معامل الانكسار، معامل الخمود، ثابت العزل الحقيقي والخيالي، التوصيلية البصرية تزداد مع زيادة تركيز جسيمات النانوية Y_2O_3. النفاذية وفجوة الطاقة للانتقال غير مباشر المسموح والممنوع تقل مع زيادة تركيز جسيمات النانوية Y_2O_3.اظهرت نتائج الخصائص الكهربائية المتناوبة (A.C) تزداد مع زيادة تركيز جسيمات النانوية Y_2O_3 وتتناقص مع زيادة تردد المجال الكهربائي المسلط. التوصيلية الكهربائية المتناوبة (AC) تزداد مع زيادة تركيز جسيمات النانوية Y_2O_3 و التردد.